The Journal of Neuroscience, September 1, 2000, *20*(17):6459–6472

Impaired Synaptic Plasticity and cAMP Response Element-Binding Protein Activation in Ca^{2+}/Calmodulin-Dependent Protein Kinase Type IV/Gr-Deficient Mice

Nga Ho,[1] Jason A. Liauw,[2] Frank Blaeser,[1] Feng Wei,[2] Silva Hanissian,[7] Lisa M. Muglia,[1] David F. Wozniak,[3] Anthony Nardi,[3] Kara L. Arvin,[1] David M. Holtzman,[4] David J. Linden,[8] Min Zhuo,[2] Louis J. Muglia,[1,5] and Talal A. Chatila[1,6]

Departments of [1]Pediatrics, [2]Anesthesiology, Anatomy and Neurobiology, [3]Psychiatry, [4]Neurology, and the Center for the Study of Nervous System Injury, [5]Molecular Biology and Pharmacology and Obstetrics and Gynecology, and [6]Pathology and Immunology, and the Center for Immunology, Washington University School of Medicine, St. Louis, Missouri 63110, [7]Division of Immunology/Rheumatology, The Children's Hospital and Department of Pediatrics, Harvard Medical School, Boston, Massachusetts 02115, and [8]Department of Neuroscience, Johns Hopkins University School of Medicine, Baltimore, Maryland 21205

The Ca^{2+}/calmodulin-dependent protein kinase type IV/Gr (CaMKIV/Gr) is a key effector of neuronal Ca^{2+} signaling; its function was analyzed by targeted gene disruption in mice. CaMKIV/Gr-deficient mice exhibited impaired neuronal cAMP-responsive element binding protein (CREB) phosphorylation and Ca^{2+}/CREB-dependent gene expression. They were also deficient in two forms of synaptic plasticity: long-term potentiation (LTP) in hippocampal CA1 neurons and a late phase of long-term depression in cerebellar Purkinje neurons. However, despite impaired LTP and CREB activation, CaMKIV/Gr-deficient mice exhibited no obvious deficits in spatial learning and memory. These results support an important role for CaMKIV/Gr in Ca^{2+}-regulated neuronal gene transcription and synaptic plasticity and suggest that the contribution of other signaling pathways may spare spatial memory of CaMKIV/Gr-deficient mice.

Key words: calcium/calmodulin-dependent kinase; synaptic plasticity; LTP; LTD; CREB; memory

Ca^{2+} signaling pathways play a pivotal role in synaptic plasticity and memory formation (Dubnau and Tully, 1998; Silva et al., 1998; Mayford and Kandel, 1999). Elevation of intracellular Ca^{2+} is necessary for the induction of different forms of synaptic plasticity, including long-term potentiation (LTP) and long-term depression (LTD), which are proposed to be important for the formation of long-term memory (LTM). In particular, later phases of LTP/LTD require activation of Ca^{2+}-dependent gene transcription, whereas manipulations that interfere with Ca^{2+} entry disrupt both synaptic plasticity and LTM responses (Chen and Tonegawa, 1997).

Several transducers of Ca^{2+} signaling have been implicated in synaptic plasticity and LTM. These include the Ca^{2+}/calmodulin-dependent protein kinase type II (CaMKII), the inactivation or antagonization of which impairs LTP in hippocampal CA1 neurons and compromises spatial memory (Silva et al., 1992a,b; Bach et al., 1995; Mayford et al., 1996; Cho et al., 1998; Giese et al., 1998). Ca^{2+}/calmodulin-dependent adenylyl cyclases also promote synaptic plasticity, learning, and memory via activation of cAMP-regulated protein kinase A (PKA) and the transcription factor cAMP response element binding protein (CREB), which PKA phosphorylates on the regulatory Ser133 residue (Shaywitz and Greenberg, 1999). Inactivation or antagonization of Ca^{2+}/calmodulin-dependent adenylyl cyclases, CREB, or PKA results in impaired LTP and LTM (Bourtchuladze et al., 1994; Qi et al., 1996; Abel et al., 1997; Wong et al., 1999).

Received Jan. 21, 2000; revised May 1, 2000; accepted June 22, 2000.

This work was supported by grants from the American Cancer Society (T.A.C.), National Institutes of Health (NIH), Howard Hughes Medical Institutes, and Monsanto Company, and a Burroughs Wellcome Fund Career Development Award in the Biomedical Sciences (L.J.M), from NIH and the Develbis fund (D.J.L.), and from the Alzheimer's Disease Research Center at Washington University School of Medicine (M.Z.). We thank Mike White for performing ES cell injection into blastocysts, and Jonathan Gitlin for discussions.

Correspondence should be addressed to Talal A. Chatila, Division of Immunology/Rheumatology, Department of Pediatrics, Washington University School of Medicine, 1 Children's Place, St. Louis, MO 63110. E-mail: chatila@kids.wustl.edu.

The Ca^{2+}/calmodulin-dependent protein kinase type IV/Gr (CaMKIV/Gr) is of particular interest in neuronal Ca^{2+} signaling because of its expression profile and its function as a transcriptional activator. CaMKIV/Gr is expressed in both nuclei and cytosol of neurons of several brain regions, including the cortex, cerebellum, hippocampus, and amygdala (Ohmstede et al., 1989; Jensen et al., 1991a,b; Means et al., 1991; Ohmstede et al., 1991). It activates several transcription factors, including CREB, which it phosphorylates on the regulatory Ser133 residue (Mathews et al., 1994; Sun et al., 1994), the CREB-related factor ATF-1, the MADS-box family members SRF and MEF2D, and the transcriptional coactivator p300/CREB-binding protein (CBP) (Miranti et al., 1995; Enslen et al., 1996; Sun et al., 1996; Chawla et al., 1998; Hu et al., 1999; Blaeser et al., 2000). CaMKIV/Gr also phosphorylates and regulates the function of synaptic proteins including the actin binding protein synapsin I (Ohmstede et al., 1989) and the microtubule regulator Stathmin/OP18 (Melander Gradin et al., 1997).

CaMKIV/Gr has been implicated in various aspects of neuronal Ca^{2+} signaling, including CREB phosphorylation and gene expression in response to excitatory neurotransmission (Bito et al., 1996), production of and responsiveness to neurotrophic factors (Finkbeiner et al., 1997; Shieh et al., 1998; Tao et al., 1998), and synaptic plasticity (Ahn et al., 1999). Notwithstanding these findings, the role of CaMKIV/Gr in neuronal Ca^{2+} signaling remains unclear and at times in dispute (Impey et al., 1998). In this study, we report on the derivation and use of CaMKIV/Gr-deficient mice to elucidate the contributions of CaMKIV/Gr to Ca^{2+}-regulated adaptive neuronal responses, including synaptic plasticity, gene expression, and learning and memory.

MATERIALS AND METHODS

Generation of CaMKIV/Gr knockout *mice*

Genomic DNA fragments spanning CaMKIV/Gr exon III were isolated by screening a genomic DNA library derived from the mouse strain L129 with the entire murine CaMKIV/Gr cDNA. A 16.5 kb genomic DNA clone was isolated that comprised the 79-bp-long CaMKIV/Gr exon III and its

surrounding intronic sequences. A 2.9 kb fragment flanking 5′ to the targeted exon was derived by cutting clone 2.17 with *Not*I (N) and *Xho*I (X), then ligated into unique *Not*I/*Xho*I sites 5′ of the neomycin resistance gene of pPNT (Tybulewicz et al., 1991). A 7.5 kb genomic fragment flanking 3′ to the target was cut out with *Bgl*II (Bgl) and *Sac*I (S) and ligated into pBluescript KS±. The insert was then cut with *Eco*RI to liberate a 6.1 kb fragment that was subcloned into the *Eco*RI site of pPNT.

The targeting plasmid was introduced by electroporation into RW4 embryonic stem (ES) cells (Genome Systems, St. Louis, MO). These were then grown on murine embryonic fibroblasts in the presence of leukemia inhibitory factor and subjected to double selection with G418 at 200 μg/ml and ganciclovir at 2.0 μM. Double drug-resistant colonies were screened for homologous recombination by Southern blotting using as a probe a 400 bp *Eco*RI fragment immediately distal to the 3′ flanking DNA sequence. Disruption of the targeted sequence resulted in the introduction of a *Bam*HI site present in the *neo* resistance gene, leading to a decrease in the size of the *Bam*HI fragment, which normally hybridizes with this probe from 12.5 to 7.5 kb.

Heterozygous CaMKIV/Gr-deficient ES cells were injected into C57BL/6 blastocysts that were reimplanted in pseudopregnant females. Several male chimeras were identified by agouti coat color, and those showing >80% agouti coats were mated to C57BL/6 females. Agouti offsprings were screened for heterozygotes (HET) by Southern blot and PCR analysis, and HET animals were bred to generate F2 hybrid homozygous-deficient (KO) mice and wild-type (WT) littermate controls. F2 hybrid siblings were used for all of the behavioral studies and most of the other experiments except where indicated. The mice used in these studies were housed on a 12 hr light/dark cycle with *ad libitum* access to rodent chow. All mouse protocols were in accordance with National Institutes of Health guidelines and approved by the Animal Care and Use Committee of Washington University School of Medicine.

RT-PCR analysis

cDNA was derived from total brain RNA of WT, HET, and KO mice by reverse transcription using an oligo dT primer, then subjected to RT-PCR analysis using the following exon III sequence flanking primers: 5′-TCCTCTGGGCGATTTCTTCG-3′ (sense primer; bp 153–172 of murine CaMKIV/Gr cDNA) and 5′-CTGATTTCTGTGGGGGTTTCG-3′ (antisense primer; bp 377–357 of CaMKIV/Gr cDNA) (Jones et al., 1991).

Histological and immunohistochemical analysis

For histological analysis, freshly dissected brains of adult KO mice and WT littermate controls were fixed overnight in phosphate-buffered 4% paraformaldehyde, embedded, and cut into 10 μM sections that were subjected to Giemsa staining after standard procedures. For immunohistochemistry, paraformaldehyde-fixed brains or hippocampal slices of adult male CaMKIV/Gr KO mice and their WT littermate controls were cryoprotected for 48 hr in 10% sucrose in Dulbecco's PBS (D-PBS). Immunohistochemical analysis was performed on free-floating sections cut at 35 μm on a cryostat. After blocking in 3% normal goat serum in PBS for 30 min, sections were incubated with a 1:1000 dilution of murine monoclonal anti-calbindin antibody (CL300; Sigma, St. Louis, MO), a 1:1000 dilution of a polyclonal rabbit anti-pCREB antibody (New England Biolabs), or a 1:20,000 dilution of a polyclonal rabbit anti-c-Fos antibody (Calbiochem, La Jolla, CA), as indicated. Antibody incubations were performed in D-PBS with 1% goat serum, and immunoreactivity was visualized using a peroxidase Vectastain Elite ABC kit (Vector Laboratories, Burlingame, CA). Staining intensity was quantitated using NIH Image software and analyzed for statistical significance between genotypes by ANOVA.

Hippocampal electrophysiology

Male WT and CaMKIV/Gr KO littermate mice at 6–8 weeks of age were anesthetized with inhaled halothane. Transverse slices of hippocampus were rapidly prepared and maintained in an interface chamber at 28°C, where they were subfused with artificial CSF (ACSF) consisting of (in mM): 124 NaCl, 4.4 KCl, 2.0 $CaCl_2$, 1.0 $MgSO_4$, 25 $NaHCO_3$, 1.0 Na_2HPO_4, and 10 glucose, bubbled with 95% O_2 and 5% CO_2. The protocol of electrical stimulation and recordings has been described (Brandon et al., 1995; Qi et al., 1996; Zhuo et al., 1999). Slices were kept in the recording chamber for at least 2 hr before the experiments. A bipolar tungsten stimulating electrode was placed in the stratum radiatum in the CA1 region, and extracellular field potentials were also recorded in the stratum radiatum using a glass microelectrode (3–12 MΩ, filled with ACSF). Stimulus intensity was adjusted to produce a response of ~1 mV amplitude. Test responses were elicited at 0.02 Hz. LTP was induced using three different paradigms: stimulations of one train (100 Hz for 1 sec), two tetanic trains (two 100 Hz, 1 sec trains at 20 sec intervals), and four tetanic trains (four 100 Hz, 1 sec trains at 5 min intervals). Most LTP recordings were performed using F2 hybrid WT and KO littermate mice with the following exception. Additional LTP recordings were generated using three WT mice and three littermate KO mice derived from matings of F6 HET parents on a C57BL/6 background. Because the latter results were not significantly different from the previous ones, the data from the two sets of LTP studies were pooled.

Homosynaptic LTD was induced by prolonged low-frequency stimulation (1 Hz for 15 min). In some experiments, NMDA receptor-mediated EPSPs were measured after the blockade of AMPA/kainate receptors using 20 μM CNQX (for at least 30 min treatment). The Mg^{2+} concentration used in these studies is 1 mM, and the residual EPSPs were completely blocked by 100 mM AP-5, in support of NMDA receptor-mediated responses being observed. Stimulations at different intensities were used to generate the fiber volley and NMDA receptor-mediated EPSP slope plot. Data are presented as mean ± SEM. One-way ANOVA (with Duncan's multiple range test for *post hoc* comparison) and Student's *t* test were used for statistical analysis. $p < 0.05$ was considered significant.

Cerebellar LTD studies

Mouse embryonic cerebellar cultures were prepared and maintained as described previously (Linden, 1996). After 10–16 d *in vitro*, perforated-patch voltage-clamp recordings were obtained. Patch electrodes attached to Purkinje neuron somata were filled with a solution containing (in mM): 95 Cs_2SO_4, 15 CsCl, 8 $MgCl_2$, 10 HEPES, pH 7.35 with CsOH. Electrode tips were filled with a small amount of this solution, and the shanks were backfilled with this solution supplemented with amphotericin B at a concentration of 300 μg/ml. Stable access resistance of <12 MΩ could be obtained within 10 min of gigaseal formation. A holding potential of −70 mV was imposed. Iontophoresis electrodes (1 μm tip diameter) were filled with 10 mM glutamate (in 10 mM HEPES, pH 7.1 with NaOH) and positioned ~20 μm away from large-caliber dendrites. Test pulses of glutamate were delivered using negative current pulses (600–900 nA, 40–110 msec duration, 0.05 Hz). After acquisition of baseline responses, six conjunctive stimuli were applied, each consisting of a glutamate test pulse combined with a 3-sec-long depolarization step to 0 mV. Cells were bathed in solution containing (in mM): 140 NaCl, 5 KCl, 2 $CaCl_2$, 0.8 $MgCl_2$, 10 HEPES, 10 glucose, 0.0005 tetrodotoxin, and 0.02 picrotoxin, adjusted to pH 7.35 with NaOH, which flowed at a rate of 0.5 ml/min. Experiments were conducted at room temperature. Bis-fura-2 ratio imaging of intracellular free Ca was accomplished by measuring the background-corrected fluorescence ratio at 340 and 380 nm excitation using a cooled CCD camera system as described previously (Linden, 1996).

Derivation and stimulation of primary cortical neuronal cell cultures

Primary murine neuronal cultures were prepared as described (Dugan et al., 1999) from neocortices of embryonic day 14 (E14) fetuses conceived by mating CaMKIV/Gr HET mice (F6 generation on C57BL/6 background). Two cultures were derived from each fetal brain, one to serve as a control and the other as the test sample. Neuronal cultures derived from fetuses of the same litter were tested in a blinded fashion, and their CaMKIV/Gr status was later established by genotyping and CaMKIV/Gr immunoblotting. Neurons were cultured in serum-free medium overnight before stimulation, then either sham-treated or depolarized by treatment with 60 mM KCl for 10 min. The cells were then lysed with 1× boiling sample buffer and boiled for 10 min. Protein concentrations of the respective samples were determined, and 12.5 μg protein of each lysate sample were loaded and resolved on 10% SDS-polyacrylamide gels, using a standard SDS-PAGE protocol. The gels were then transferred to nitrocellulose membranes and subjected to immunoblotting.

Immunoblotting

Whole brain and testis homogenates were derived from dissected brains and testes of adult WT, HET, and KO littermate mice using a Polytrone homogenizer. Homogenates were cleared by high-speed centrifugation, and 50 μg protein samples were resolved by SDS-PAGE, then transferred to nitrocellulose membranes for immunoblotting. Membranes of whole brain homogenates or neuronal cell culture lysates were blocked in fat-free milk, then probed with one or more of the following antibodies as indicated: mouse monoclonal anti-CaMKIV/Gr catalytic domain antibody, anti-CaMKIIα antibody, and anti-PKA catalytic subunit (PKAc) antibody (Transduction Laboratories); goat polyclonal anti-CaMKIV/Gr c-terminal peptide antibody, rabbit polyclonal anti-ERK antibody, and mouse monoclonal anti-Rsk-2 or anti-CREB antibodies (Santa Cruz Biotechnology); and phospho-specific anti-ERK (pERK) and anti-CREB (pCREB) antibodies (New England Biolabs). The blots were developed using horseradish peroxidase-conjugated secondary antibodies and enzyme-linked chemiluminescence (ECL, Amersham, Arlington Heights, IL).

pCREB and c-Fos induction by glutamate-perfusion and restraint-stress paradigms

For pCREB and c-Fos staining of glutamate-perfused hippocampal slices, the latter were prepared and maintained for 2 hr in an interface chamber at 28°C subfused with ACSF. They were then perfused with sodium glutamate (100 μM) for the indicated periods after which they were fixed in paraformaldehyde and analyzed as indicated above. For pCREB staining in the context of restraint-stress, adult male CaMKIV/Gr KO mice and their WT littermate controls were either left unhandled or subjected to 30 min of restraint-stress, then processed either immediately or 2 hr thereafter. Mice were anesthetized with 1 ml of 2.5% Avertin and transcardially perfused with D-PBS followed by 4% paraformaldehyde in D-PBS and processed for pCREB staining as described above. Analysis of c-Fos induction on restraint-stress was performed as above except that the mice

were restrained for 1 hr and then returned to their cages for 2 hr before they were killed and analyzed. Staining intensity was quantitated using NIH Image software and analyzed for statistical significance between genotypes by ANOVA.

Behavioral analyses

F2 hybrid CaMKIV/Gr KO mice ($n = 14$) and WT littermate controls ($n = 12$) that were 3–4 months of age when behavioral testing began were evaluated for the following tests. All tests were performed in a blinded fashion.

One hour locomotor activity test. Testing was performed in transparent (47.6 × 25.4 × 20.6 cm high) polystyrene cages. Movement was monitored by photocells, and their output was fed to an on-line computer (Hamilton-Kinder, LLC, Poway, CA). The system software (Hamilton-Kinder, LLC) was used to define a 33 × 11 cm central zone and a peripheral or surrounding zone that was 5.5 cm wide with the sides of the cage being the outermost boundary. Variables that were analyzed included the total number of ambulations, number of entries, time spent, and distance traveled in the center area and the distance traveled in the periphery. Testing took place between 7:30 A.M. and 3 P.M. in a quiet room continuously illuminated by fluorescent lights.

Sensorimotor battery. The general sensorimotor capabilities of the mice were evaluated using the four tests described below according to previously published methods (Wozniak et al., 1990; Brosnan-Watters et al., 1996, 1999). The inclined screen test involved placing mice on an elevated wire mesh grid (16 squares per 10) that was stretched across a wooden frame that was 15 × 52 cm and inclined to 60°. Each mouse was placed in the middle of the screen with its head oriented downward and scored for either how long it remained on the screen or how long it took to turn 180° and climb to the top of the apparatus and rest its forepaws on top. A maximum score of 60 sec was given if an animal did not fall. In the platform test, each mouse was timed for how long it remained on an elevated (47 cm above the floor) circular platform (1.0 cm thick, 3.0 cm diameter). A maximum score of 60 sec was assigned if the mouse remained on the platform for the duration of that time or if it could climb down, without falling, on a very thin pole that supported the platform. For the ledge test, each mouse was timed for how long it could maintain its balance on a narrow (0.75 cm thick) Plexiglas ledge without falling (60 sec maximum). A score of 60 sec was also assigned if the mouse traversed the entire length (51 cm) of the Plexiglas ledge and returned to the starting place under 60 sec without falling. For the walking initiation test, mice were placed in the middle of a square outlined by white cloth tape (21 × 21 cm) on a smooth black surface of a large table top. The time it took each mouse to leave the square (place all four paws outside of the tape) was recorded, with a maximum time of 60 sec allowed.

Accelerating rotorod test. Mice were tested for their ability to maintain balance on a rotating rod (rotorod) that gradually increased its rotational speed over time. The protocol consisted of two phases: habituation/adaptation (3 d) and accelerated rotorod testing (5 d). During habituation/adaptation, the mice were trained to remain on a stationary rod (3 cm diameter) on day 1 and then on the same rod when it was rotated at a constant speed (2.5 rpm) on days 2 and 3. Training on the rod that rotated at a constant speed involved two daily sessions, each containing three consecutive 1 min trials with a 10 min interval separating the two sessions. Two days after completing habituation/adaptation, the mice were evaluated on the accelerating rotorod test, which involved quantifying how long mice could remain on the rod when its rotational speed was accelerated from 2.5 to 20 rpm in 3 min. Each of the five daily test sessions consisted of three, 3 min trials, and each trial was separated by 10 min. The time the mice spent on the rod without falling was recorded for each trial.

Morris water navigation task. Mice were trained in a round pool of opaque water to learn the location of a platform that could be used to escape out of the water. The pool was 100 cm in its inner diameter, 20.5 cm deep, was filled to a depth of 17.5 cm with water maintained at a temperature of 24 ± 1°C, and was located in the center of a room containing many distinct distal spatial cues. All trials were videotaped with an overhead camera. The paths of the mice were recorded by a computerized tracking system (Polytrack, San Diego Instruments, San Diego, CA) that was used to calculate the escape latency (latency to find the platform) and distance traveled (path length) to reach the platform for each trial. Mice were trained under three different conditions conducted in the following order: (1) cued condition (visible platform, variable location), (2) place condition (submerged platform, fixed location), and (3) reversal condition (submerged platform, fixed location but different from place trials location).

To evaluate the possibility that non-associative factors might affect spatial learning/memory performance, mice were first tested in the "cued" condition in which they were trained to learn the location of a "visible" platform. In the cued condition, the platform was submerged beneath the surface of the water, but its location was made apparent by a rod that was screwed into the base of the platform and protruded 20 cm above the water surface. A red tennis ball was attached to the rod to heighten the salience of the cue denoting the position of the platform. To minimize reliance on spatial cues, the platform was pseudorandomly placed once into each of the four quadrants [N, S, E, and W (compass points)] during each block of four trials and never appeared in the same quadrant on consecutive trials. Release points (NE, SE, SW, and NW) were pseudorandomly assigned in the same manner. In the cued condition, the mice remained on the platform for 5 sec and then were placed in a holding cage for 5 sec, for a total inter-trial interval of 10 sec. Mice were tested for 3 consecutive days, and each day the mice received two sets of two consecutive 60 sec trials separated by 1 hr of rest, for a total of 12 trials for the cued condition (three blocks of four trials each) of escape latency and path length.

Three days after completing the cued trials, the mice were trained in the "place" condition to learn the location of a platform that was submerged 1.5 cm beneath the surface of the water and located 15 cm from the wall of the pool. For the place condition, the rod/ball assembly was removed from the base of the platform, and for each mouse the location of the escape platform was randomly assigned to one of the four pool quadrants (N, S, E, or W), where it remained for all of the place trials. Release points (NE, SE, SW, and NW) were pseudorandomly assigned with one point being designated for each trial within a block of four trials and so that the same release point was never used on two consecutive trials. The mice received 5 d of training in the place condition. On day 1, testing began after a pretest acclimation period, during which a mouse was placed on the platform in the pool for 30 sec and then in a holding cage for 30 sec. After pretest acclimation, each mouse underwent four consecutive trials. After each trial, a mouse remained on the platform for 30 sec and was then placed into a holding cage for 5 sec, followed by the next trial, making for a total inter-trial interval of 35 sec for the place trials. On days 2–5, the mice received four consecutive place trials on each day. Day 3 ended with a 60 sec "probe" trial, during which the escape platform was removed from the pool and the mouse was released into the maze at a point that was diagonally opposite from the previous location of the platform. The time spent searching in the target quadrant where the platform had been located, the number of crossings over the former platform location (platform crossings), and the percentage of total distance traveled in the target quadrant were recorded. Another probe trial was given the day after the last test day (i.e., on day 6).

Two days after the second probe trial of the place condition, mice were trained over 5 d on the "reversal" place learning condition during which the platform was moved to the quadrant diagonally opposite its previous location. Just before the first trial of the reversal phase, each mouse was acclimated to the platform's new location for 30 sec. During reversal training, the mice received two consecutive trials followed by a 1 hr rest period and then two more consecutive trials. Probe trials were given at the end of day 4 and 3 d after day 5 of reversal training. Other aspects of reversal training were similar to those used during the original place phase. A total of 20 trials (five blocks of four trials) of escape latency and path length data as well as data from two probe trials were collected for both the place and the reversal conditions. In addition, mean swimming speed scores were computed for each day within all three test conditions (cued, place, and reversal) by dividing the mean escape latency for a given day by the mean path length for that day. Swimming speed scores were calculated to provide an additional measure for comparing the swimming capabilities of the two groups.

Radial arm maze. Mice were food-restricted to ~85% of their *ad libitum* weight and trained on the win-shift spatial discrimination in the radial arm maze to evaluate working (trial-dependent) memory according to previously published procedures (Wozniak et al., 1990). The food reward that was used during testing (Fruity Pebbles cereal) was introduced into the cages of the mice a week earlier so that they would become familiar with it. The maze consisted of an octagonal central platform enclosed by a Plexiglas frame that contained eight experimenter-controlled doors that block access to the eight arms. The mice were habituated to handling and the experimental procedures and were trained to traverse the arms and retrieve and consume a Fruity Pebbles tidbit placed in a cup at the end of each arm. Neophobia was assessed by recording the time it took a mouse to first begin eating the Fruity Pebbles tidbits spread throughout the maze during the first 2 d of shaping. In the last phase of habituation, one Fruity Pebbles tidbit was placed in each arm and a mouse qualified for acquisition training when it ate all eight Fruity Pebbles within 5 min on 2 of 3 consecutive days. Acquisition involved baiting each arm with a Fruity Pebbles tidbit and training a mouse to traverse each baited arm and consume the reinforcer (a correct response) and to remember the arms that it had been reinforced in so that it would not revisit those arms (commit a retracing error). Acquisition was defined by an a priori criterion of at least eight correct responses of the first nine responses for 4 consecutive days. Days and errors to criterion served as dependent variables for evaluating acquisition performance.

Statistical analyses for the behavioral tests. The data from the behavioral tests were analyzed using ANOVA models. In some instances, one-way ANOVAs were conducted for a given variable or test, e.g., number of entries into the central zone of the open field or number of total ambulations. In other instances such as for the variables generated in the Morris water navigation or radial arm maze tasks, two-way ANOVAs were used for a given variable that contained one between-subjects variable, group (CaMKIV/Gr KO vs WT) and one within-subjects variable, such as blocks of trials or test days. Simple main effects of group or other contrasts were conducted after a significant main effect of group or a significant group by blocks of trials or test days interactions. α levels were adjusted for within-subjects variables containing more than two levels using the Huynh-Feldt correction to control for violations of sphericity/compound symmetry.

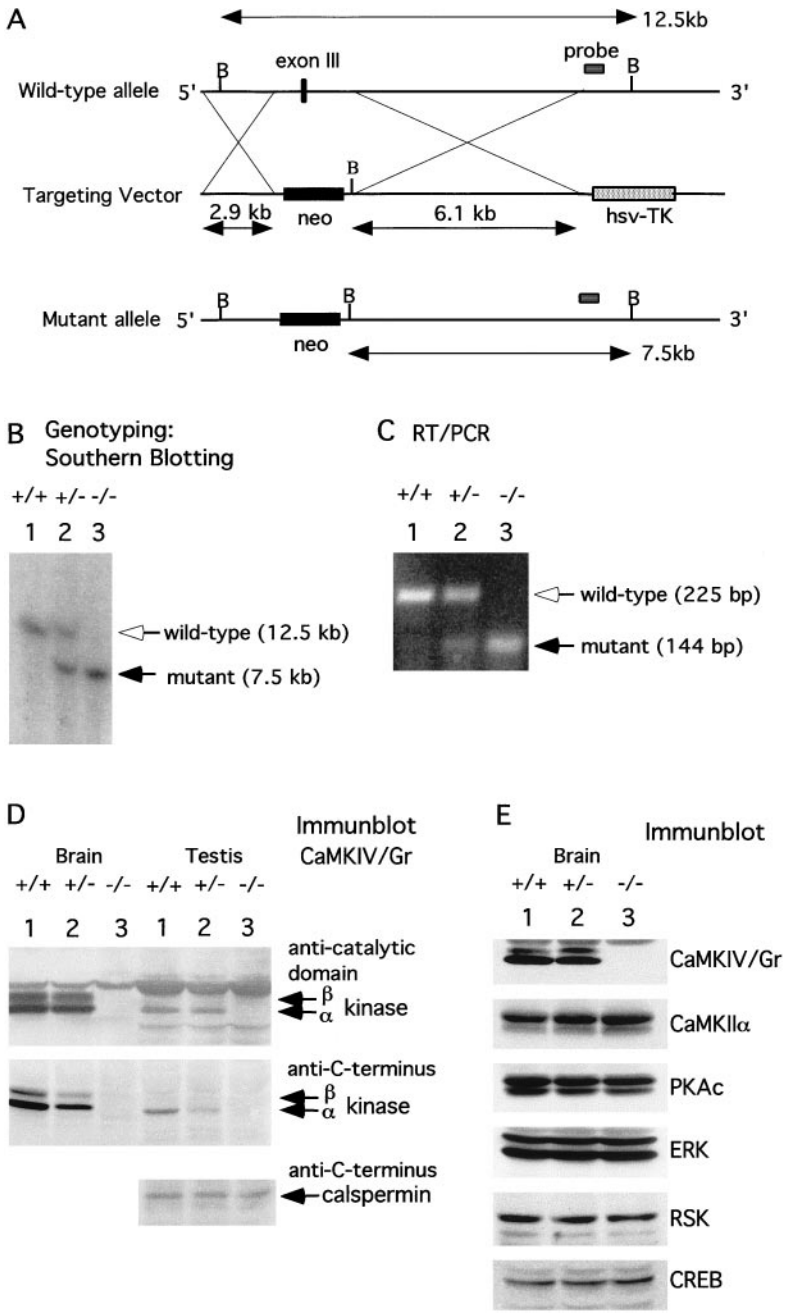

Figure 1. Targeted disruption of a murine CaMKIV/Gr gene. *A*, Targeting strategy. A 16.5 kb murine genomic DNA clone composed of the 79-bp-long CaMKIV/Gr exon III and its surrounding intronic sequences was isolated and used for targeting construct preparation. A 2.9 kb and a 6.1 kb genomic fragment flanking 5′ and 3′ to the targeted exon, respectively, were derived and inserted into the targeting vector pPNT, which was used to replace exon III with a *neo* cassette. The introduction by homologous recombination of a *Bam*HI site found next to the *neo* cassette converts a 12.5 kb *Bam*HI genomic fragment spanning CaMKIV/Gr exon III in the WT allele into a 7.5 kb fragment in the mutant allele. *B* indicates *Bam*HI sites, and *hsv-TK* denotes the herpes simplex virus thymidine kinase gene that was used for negative selection with ganciclovir. *B*, Southern blot analysis of mouse tail DNA derived from WT (+/+) (*lane 1*), HET (+/−) (*lane 2*), and KO (−/−) (*lane 3*) mice. DNA was digested with *Bam*HI and subjected to hybridization using a genomic DNA probe 3′ to the targeting construct, which is depicted in *A*. *C*, RT-PCR analysis of brain-derived CaMKIV/Gr transcripts of WT, HET, and KO mice using exon III-flanking oligonucleotides. WT transcripts give rise to a 223 bp fragment, whereas exon III-deficient transcripts give rise to a 144 bp fragment. *D*, Immunoblot analysis of CaMKIV/Gr expression in brain and testicular tissues of WT and mutant mice using a monoclonal antibody directed against the catalytic domain or an antiserum directed at the C-terminal peptide of the murine kinase that will also detect calspermin. CaMKIV/Gr is expressed as two isoforms (α/β) derived from the same gene that are indicated by *double arrows*. Both isoforms were absent in KO mice. The testis-specific protein calspermin, which is composed of the calmodulin-binding and the C-terminal domains of CaMKIV/Gr, is detected by the anti-CaMKIV/Gr C-terminal peptide antiserum and was found to be equally expressed in WT and mutant mice (*D*). *E*, CaMKIV/Gr deficiency does not alter the expression of CREB or of other CREB kinases. Immunoblots were performed on samples of whole-brain homogenates of WT (+/+), HET (+/−), and KO (−/−) mice using antibodies specific for CaMKIV/Gr, CaMKIIα, PKA catalytic subunit (PKAc), Rsk-2, ERK1 and 2, and CREB.

RESULTS

Generation of CaMKIV/Gr-deficient mice

The CaMKIV/Gr gene includes 13 exons that extend over at least 42 kb of DNA (Sun et al., 1995). It encodes three proteins, the α and β isoforms of CaMKIV/Gr and calspermin, that are derived by alternative transcriptional initiation and alternative splicing (Ohmstede et al., 1991; Sun et al., 1995). Our targeting strategy aimed to disrupt CaMKIV/Gr-α and -β expression while sparing that of calspermin by avoiding targeting of any of the promoter sequences of the gene or calspermin coding sequences. To this end, a targeting vector was constructed that was designed to replace the 79 bp exon 3 of CaMKIV/Gr (encoding the ATP binding site in the catalytic domain of the kinase) with a phosphoglycerate kinase-neomycin resistance cassette (Fig. 1*A*). Replacement of CaMKIV/Gr exon III with a neomycin resistance gene was predicted to result in the generation of out of frame, alternatively spliced kinase transcripts that skip the inserted neomycin cassette and encode a catalytically inactive 55 amino acid peptide before terminating at a premature stop codon. On the basis of our previous studies on N-terminal, catalytically inactive CaMKIV/Gr fragments, such a peptide would fail to be expressed in targeted cells because of instability/degradation (Chatila et al., 1996).

Three of 83 G418 and ganciclovir-resistant ES clones underwent homologous recombination as determined by Southern blot analysis using a hybridization probe external to the region of homology contained within the targeting vector. Several male chimeras were generated from two ES clones that transmitted the mutant allele through the germline. Matings of CaMKIV/Gr HET mice resulted in generation of CaMKIV/Gr KO mice (Fig. 1*B*) in numbers consistent with autosomal recessive Mendelian inheritance (data not shown). KO mice of both sexes were grossly indistinguishable from their WT and HET littermates and were fertile.

Northern blot analysis revealed equivalent levels of CaMKIV/Gr transcripts in brains, testes, and thymi of WT and mutant animals (data not shown). However, RT-PCR analysis using flanking primers confirmed the absence from transcripts of

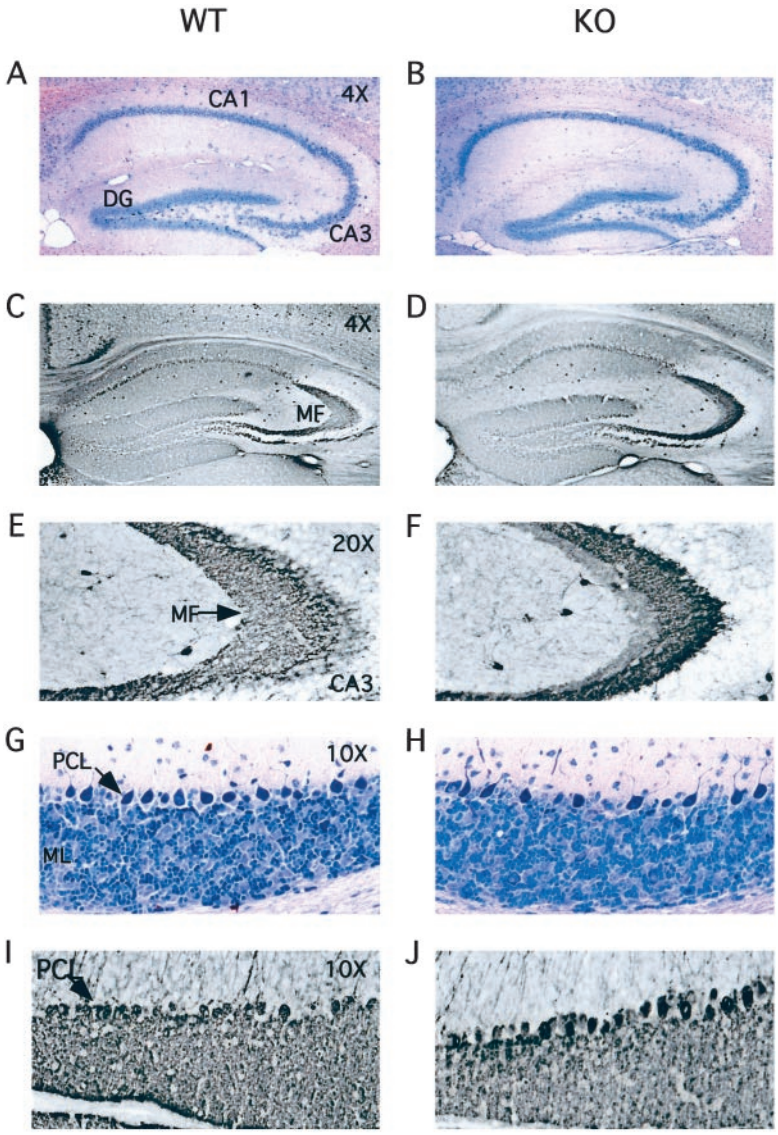

Figure 2. Hippocampal and cerebellar morphology of WT and CaMKIV/Gr KO mice. *A*, *B*, Giemsa staining of the hippocampal formation of WT (*A*) and CaMKIV/Gr KO (*B*) littermate mice. Areas CA1 and CA3 as well as the dentate gyrus (*DG*) are indicated (4× magnification). *C*, *D*, Calbindin immunostaining of the hippocampus of WT (*C*) and CaMKIV/Gr KO mice (*D*). Mossy fiber tract (*MF*) is visualized (4× magnification). *E*, *F*, A higher magnification view (20×) of calbindin-stained mossy fiber tracts of WT (*E*) and KO (*F*) mice (corresponding to *C* and *D*, respectively). *G*, *H*, Giemsa staining of the cerebellum of WT (*G*) and CaMKIV/Gr KO (*H*) littermates. *PCL*, Purkinje cell layer; *ML*, molecular layer. *I*, *J*, Calbindin immunostaining of WT (*I*) and CaMKIV/Gr KO (*J*) cerebella. Purkinje cell dendritic arborization is visualized as a thick interlacing web underneath the Purkinje cell layer.

KO mice of targeted exon III sequence, whereas HET mice manifested both WT and exon III-deficient transcripts (Fig. 1*C*). Expression of CaMKIV/Gr protein in targeted animals was evaluated by immunoblotting using two different anti-CaMKIV/Gr antibodies: one directed at the C-terminal peptide and the other at the catalytic domain (Fig. 1*D*). In both cases, CaMKIV/Gr protein expression was found to be totally absent in KO mice and reduced by 50% in HET mice as compared with WT littermates. In contrast, expression of the testis-specific calspermin protein, as detected by the anti-CaMKIV/Gr C-terminal peptide antibody, was normal (Fig. 1*D*). Similarly, there was normal expression in CaMKIV/Gr KO mice of other protein kinases such as CaMKIIα, ERK1 and 2, RSK-2, and PKA, and of the CaMKIV/Gr substrate CREB (Fig. 1*E*).

To determine whether CaMKIV/Gr deficiency causes gross neuroanatomical abnormalities, we compared coronal sections from brains of WT and KO mice using different stains (Fig. 2). Histological analysis revealed the gross hippocampal morphology of WT and KO mice to be indistinguishable. Giemsa (Fig. 2*A*,*B*) and Nissl (data not shown) staining revealed the cellular composition and orientation of different hippocampal substructures to be comparable in WT and KO mice (Fig. 2*A*,*B*). The neocortex showed the normal layered structure (data not shown). Calbindin immunostaining revealed apparently normal mossy fiber projections to the CA3 (Fig. 2*C–F*). Cerebellar histology appeared grossly normal (Fig. 2*G*,*H*), and calbindin immunostaining visualized Purkinje cell dendritic arborization in both WT and KO animals (Fig. 2*I*,*J*).

Impaired LTP in CA1 neurons of CaMKIV/Gr KO mice

To address the role of CaMKIV/Gr in synaptic plasticity at the Schaffer collateral/CA1 synapse in the hippocampus, we examined two major forms of synaptic plasticity: LTP and LTD. First, we examined the competency of basal synaptic transmission in hippocampal slices of WT and KO mice. Paired-pulse facilitation, a simple form of plasticity, in KO slices was similar to that of WT controls at different intervals measured (WT: $n = 15$ slices/8 mice; KO: $n = 13$ slices/9 mice) (Fig. 3*A*). No obvious difference in baseline EPSPs was observed in slices of WT and KO mice (data not shown). To test whether NMDA receptor-mediated responses may be affected in KO mice, we measured NMDA receptor-mediated field EPSPs in the presence of AMPA/kainate receptor blockade (CNQX, 20 μM). We found that NMDA receptor-mediated responses in hippocampal slices of KO mice were not significantly different from those of WT mice (WT: $n = 11$ slices/7 mice; KO: $n = 5$ slices/5 mice) (Fig. 3*B*).

Next we examined LTP induction in hippocampal slices of WT and KO mice after tetanic stimulation. Strong tetanic stimulation (two trains, 100 Hz for 1 sec/train, delivered at a 20 sec interval) (Zhuo et al., 1999) induced robust and sustained potentiation of synaptic responses ($n = 7$ slices/7 mice, 241.7 ± 18.5% of control,

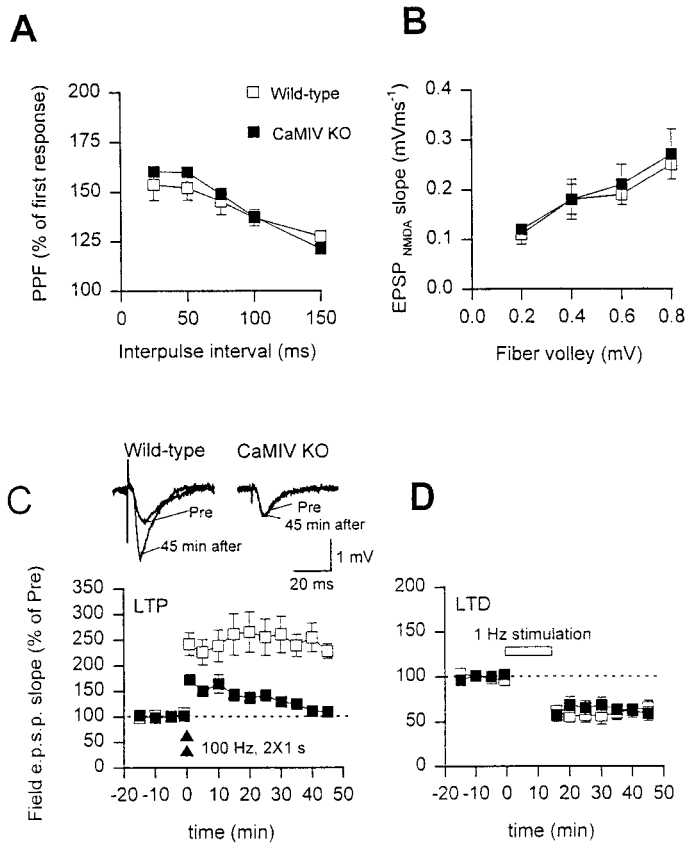

Figure 3. Impaired LTP but normal LTD in CA1 neurons of CaMKIV/Gr KO mice. *A*, WT and KO hippocampal slices show no significant difference in paired-pulse facilitation (PPF) of the EPSPs at various interpulse intervals (WT: $n = 15$ slices/8 mice; KO: $n = 13$ slices/9 mice). *B*, WT and KO hippocampal slices show no significant difference in NMDA receptor-mediated EPSPs (WT: $n = 11$ slices/7 mice; KO: $n = 5$ slices/5 mice). *C*, LTP induced by two-train tetanic stimulation was blocked in slices of CaMKIV/Gr KO mice (WT: $n = 7$ slices/7 mice, 241.7 ± 18.5% of control, comparing 45 min after strong tetanus to before stimulation, $p < 0.05$; KO: $n = 12$ slices/9 mice, 109.0 ± 9.2.0%). Representative field EPSP (fEPSP) traces before and 45 min after stimulation are shown in the *insets*. *D*, LTD is normal in CaMKIV/Gr KO mice. Low-frequency stimulation (1 Hz, 15 min) induced LTD in the CA1 region of the hippocampus from WT mice (□; $n = 6$ slices/6 mice, 59.7 ± 7.1% of control, comparing 40–45 min after 1 Hz stimulation with before the stimulation, $p < 0.05$) or KO mice (■; $n = 8$ slices/8 mice, 60.2 ± 8.0% of control, $p < 0.05$).

comparing 45 min after strong tetanus to before stimulation, $p < 0.05$) (Fig. 3*C*). However, no significant potentiation was observed in slices from KO mice 45 min after identical tetanic stimulation ($n = 12$ slices/9 mice, 109.0 ± 9.2.0%). Early potentiation, however, was still observed in these slices (Fig. 3*C*). Long-term synaptic depression induced by prolonged low-frequency stimulation (1 Hz, 15 min) (Dudek and Bear, 1992; Brandon et al., 1995) was also studied in both WT and knockout mice (Fig. 3*B*). Interestingly, 1 Hz stimulation induced a similar amount of depression in slices of WT mice ($n = 6$ slices/6 mice, 59.7 ± 7.1% of control, comparing 40–45 min after 1 Hz stimulation to before the stimulation; $p < 0.05$) and KO mice ($n = 8$ slices/8 mice, 60.2 ± 8.0% of control; $p < 0.05$) (Fig. 3*D*). These results indicate that the defect in synaptic plasticity in KO mice is selective for potentiation but not depression in the hippocampus.

Hippocampal LTP can be dissociated into a transient (or early), protein synthesis-independent phase (E-LTP) lasting for up to 1 hr and a sustained (or late) phase (L-LTP) that is protein synthesis dependent and lasts for up to several days (Frey et al., 1988, 1993; Huang and Kandel, 1994; Nguyen et al., 1994). The former can be recapitulated by a single high-frequency tetanic stimulation, whereas the latter requires multiple-train tetanization (Huang and Kandel, 1994). To test whether the defect in synaptic potentiation

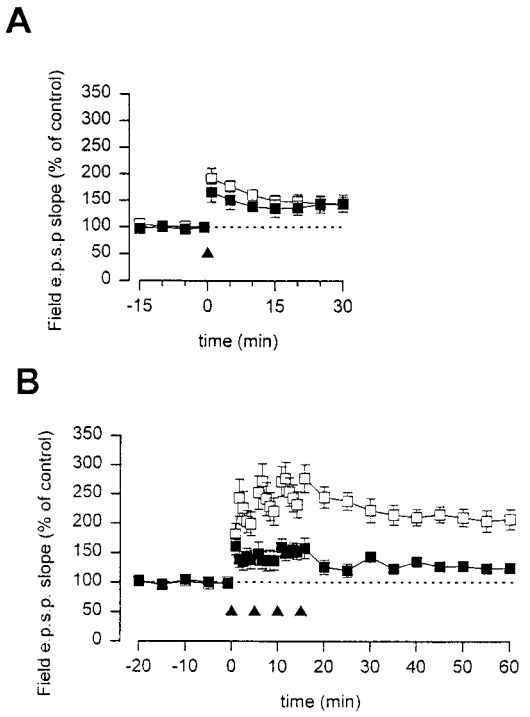

Figure 4. LTP deficiency is not overcome by multiple-train stimulation of hippocampal slices of KO mice. *A*, Synaptic potentiation induced by one-train tetanic stimulation (100 Hz for 1 sec) showed no significant change in KO versus WT mice at 30 min after stimulation (WT: $n = 10$ slices/9 mice, 144.1 ± 16.4%; KO: $n = 8$ slices/8 mice, 142.9 ± 13.6%). *B*, Late-phase LTP induced by four-train tetanic stimulation (100 Hz for 1 sec, delivered 4 times at 5 min intervals) was significantly decreased in KO mice at 60 min (WT: $n = 7$ slices/7 mice, 205.0 ± 18.2%; KO: $n = 6$ slices/6 mice, 125.0 ± 7.2%, $p < 0.05$).

in CA1 neurons of KO mice involves both forms of LTP, we examined LTP induction in slices of WT and KO mice during single-train tetanic stimulation (100 Hz for 1 sec) as compared with multiple-train stimulation (four trains, 100 Hz for 1 sec/train, delivered at 5 min intervals) (Huang and Kandel, 1994). Although the amount of potentiation 30 min after a one-train tetanic stimulation in WT and KO mice was not significantly different (WT: $n = 10$ slices/9 mice, 144.1 ± 16.4%; KO: $n = 8$ slices/8 mice; 142.9 ± 13.6%) (Fig. 4*A*), synaptic potentiation at 60 min induced by four-train stimulations in slices of KO mice was significantly smaller than that of WT mice (WT: $n = 7$ slices/7 mice, 205.0 ± 18.2%; KO: $n = 6$ slices/6 mice, 125.0 ± 7.2%, $p < 0.05$) (Fig. 4*B*). As in the case of two-train stimulation, the defect in L-LTP induction in the four-train stimulation paradigm was notable at very early time points, even as repeat tetanization was in progress (Fig. 4*B*). These results consistently suggest that CaMKIV/Gr is critical for long-term persistence of synaptic potentiation induced by two- or four-train tetanic stimulation of hippocampal slices.

Absent late-phase LTD in cerebellar Purkinje cells of CaMKIV/Gr KO mice

Cerebellar LTD is a cellular model system of information storage that has been suggested to underlie certain forms of motor learning (for review, see Daniel et al., 1998). In cerebellar LTD, a persistent, input-specific attenuation of the parallel fiber–Purkinje neuron synapse is produced when parallel fiber and climbing fiber inputs to a Purkinje neuron are stimulated together at low frequency. Similar to hippocampal LTP, cerebellar LTD has also been demonstrated to be composed of an early, protein synthesis-independent phase lasting for 1–2 hr and a late phase that is protein synthesis dependent and lasts for several hours (Linden, 1996; Murashima and Hirano, 1999). Both CREB and CaMKIV/Gr have been implicated in the establishment of a late phase of cerebellar LTD. Particle-mediated transfection of cultured Purkinje neurons

Table 1. Effects of CaMKIV/Gr deletion on some basal properties of Purkinje neurons in culture

Measure	C57BL6 WT	CaMKIV/Gr KO
R_{input} (MΩ)	175 ± 30	458 ± 55*
mEPSC frequency (sec)	8.3 ± 2.7	2.7 ± 0.8*
mEPSC amplitude (pA)	25 ± 6	29 ± 6
Resting Ca, 2 mM external (nM)	109 ± 17	114 ± 120
Depolarization-evoked Ca_i (nM)	506 ± 54	483 ± 49
Resting Ca, 0 mM external (nM)	32 ± 8	33 ± 8
Quisqualate-evoked Ca_i (nM)	166 ± 31	175 ± 30

Values are mean ± SEM. $n = 10$ cells. R_{input} was determined by measuring the sustained current deflection during a voltage step from −80 to −90 mV. mEPSCs were measured over a 200 sec continuous interval before any additional manipulation (depolarization or quisqualate application). Bis-fura-2 microfluorimetric measurements of depolarization-evoked and quisqualate-evoked Ca were conducted in cells separate from those of the LTD experiments. Values are peak proximal dendritic Ca concentration for Purkinje neurons and peak somatic Ca for granule neurons. Depolarization-evoked Ca_i was measured in cells that were incubated in normal (2 mM Ca-containing) external saline and stimulated with a 3 sec depolarizing pulse from −80 to 0 mV. Quisqualate-evoked Ca_i, a measure of group I mGluR function, was measured in cells that were incubated in 0 Ca/0.2 EGTA external saline and stimulated with a pressure pulse of 100 μM quisqualate (dissolved in 0 Ca/0.2 EGTA saline, 4 psi, 2 sec). This pressure pulse delivered agonist to the entire cell. Resting values were measured immediately before stimulation. Depolarization-evoked values were measured as the peak during a 30 sec measuring period after the onset of depolarization, and quisqualate-evoked values were measured as the peak during a 120 sec measuring period after the onset of the pressure pulse. *$p < 0.01$ compared with WT, Student's t test.

with an expression vector encoding a dominant inhibitory form of CREB resulted in a nearly complete blockade of the late phase of LTD (Ahn et al., 1999). Also, although inhibitors of PKA or the mitogen-activated protein kinase/ribosomal 56 kinase (MAPK/RSK) cascade were without effect on the late phase, transfection with expression vectors encoding a CaMK inhibitor peptide, dominant negative forms of CaMKIV/Gr, or a calmodulin trap localized to the nucleus produced attenuation of the late phase of LTD.

As a further test of this hypothesis, LTD was assessed in cerebellar cultures prepared from CaMKIV/Gr KO mice. Because Ca^{2+} influx via voltage-gated Ca channels and activation of the glutamate receptor mGluR1 are required for LTD induction, alterations in these signals in the KO could block cerebellar LTD. However, when these functions were measured using bis-fura-2 microfluorimetry, no difference was seen between KO and WT Purkinje neurons (Table 1). Likewise, the amplitude of mEPSCs was unaltered in KO neurons. There were, however, two significant alterations in the basal physiology of KO Purkinje neurons: the frequency of mEPSCs was reduced by ~70%, and R_{input} was increased by ~250% (Table 1). Although we did not quantitate the morphology of the Purkinje neurons in culture, it appeared as if the dendritic arbors of the KO neurons were significantly reduced, and we hypothesize that this alteration could underlie both the decrease in mEPSC frequency (through a reduction in the number of synapses) and the increase in R_{input} (through a reduction in total membrane surface area).

Induction of LTD by glutamate/depolarization conjunction (six 3-sec-long depolarization steps to 0 mV, each paired with an iontophoretic glutamate pulse) in C57BL6 WT Purkinje neurons resulted in an attenuation of subsequent glutamate test pulses that persisted for the duration of the experiment (58 ± 9.2% of baseline at $t = 120$ min, $n = 7$) (Fig. 5). In contrast, when this treatment was applied to KO cultures, LTD was evoked that persisted for ~45 min and then slowly returned to baseline values (92 ± 8.0% of baseline at $t = 120$ min, $n = 9$) (Fig. 5), similar to that previously seen with protein synthesis inhibitors or nuclear removal (Linden, 1996) or transfection with dominant inhibitory CREB or CaMKIV/Gr constructs (Ahn et al., 1999). When the number of conjunctive stimuli was doubled (to 12 pairings), a similarly attenuated late phase was produced (96 ± 9.4% of baseline at $t = 120$ min, $n = 5$) (Fig. 5).

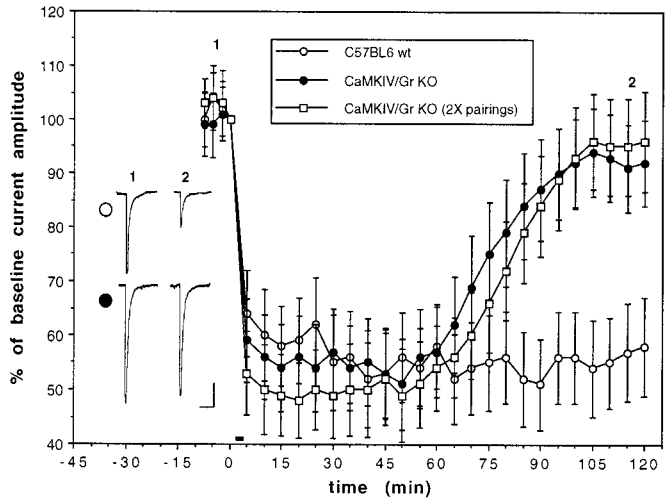

Figure 5. A late phase of cerebellar LTD is attenuated in cultured Purkinje neurons derived from CaMKIV/Gr KO mice. After acquisition of baseline responses to glutamate test pulses, glutamate/depolarization conjunction (6 pairings) is applied at $t = 0$ min. A late phase of LTD is induced in C57BL6 wt ($n = 7$) but not CaMKIV/Gr KO ($n = 9$) Purkinje neurons. Doubling the number of conjunctive pairings (2× = 12 pairings) failed to rescue the late phase in CaMKIV/Gr KO Purkinje neurons ($n = 5$). Error bars show the SEM. Representative current traces are from the time points indicated on the graph. Calibration: 30 pA, 2 sec.

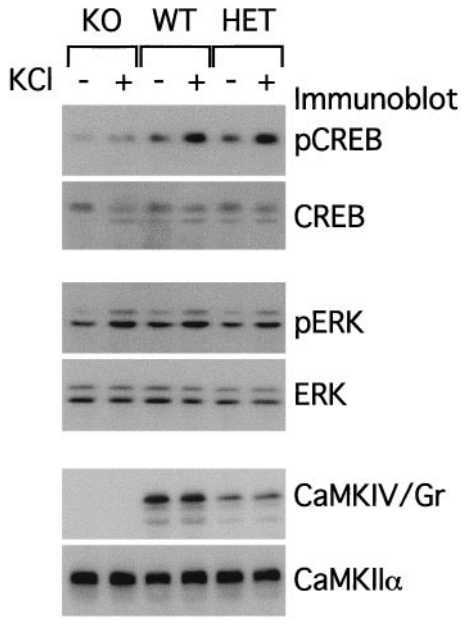

Figure 6. Decreased basal and depolarization-induced pCREB levels in primary cortical neurons of KO E14 mice relative to WT and HET littermates. Lysate samples of untreated or KCl-treated (60 mM, 10 min) neurons were immunoblotted for pCREB, total CREB, pERK, total ERK, CaMKIV/Gr, and CaMKIIα, respectively, using specific antibodies. Results are derived from a study performed in a blinded fashion on one litter. Similar results were found in an independent study on another litter.

Impaired CREB activation in CaMKIV/Gr KO mice

Because CaMKIV/Gr has been implicated as a major CREB kinase, and because CREB-dependent gene transcription has been implicated in the maintenance of synaptic plasticity, we examined CREB activation in CaMKIV/Gr KO neurons under different stimulation paradigms. First, we examined depolarization-induced pCREB formation in primary cortical neuronal cell cultures derived from E14 WT, HET, and KO littermate fetuses. Figure 6 demonstrates that KO neurons exhibited low basal pCREB levels, which increased modestly during depolarization induced by KCl

treatment. In contrast, both WT and HET neurons exhibited substantially higher basal pCREB levels, which in turn were markedly upregulated after KCl addition. The deficit in pCREB formation in KO neurons did not reflect lack or dysfunction of other CREB activation pathways, in that ERK kinase activation, monitored by staining with anti-pERK antibody, proceeded equally well in neurons of all three genotypes (Fig. 6).

Next, we examined pCREB formation in hippocampal slices of KO mice and WT littermate controls during treatment with glutamate. Immunohistochemical analysis revealed minimal pCREB staining in untreated WT and KO hippocampal slices. In contrast, glutamate treatment readily induced nuclear pCREB staining in a large number of CA1 neurons of WT slices, whereas only faint staining was observed in a limited number of CA1 neurons of KO slices (Fig. 7*A*). Similarly defective pCREB formation was also observed at an early time point (15 min) after glutamate treatment (data not shown). c-Fos expression was also examined at 45 min after glutamate treatment and was found to be greatly decreased in CA1 neurons of KO mice compared with controls (Fig. 7*B*). Image densitometric analysis confirmed the defective formation in glutamate-perfused KO CA1 neurons of both pCREB and c-Fos as compared with WT controls ($p = 0.007$ and <0.0001, respectively; $n = 4$ slices/4 animals for each group) (Fig. 7*C*). These results suggested impaired CREB activation and CREB- and Ca^{2+}-dependent gene expression in CA1 neurons of KO mice under conditions simulating excitatory neurotransmission.

To evaluate CREB activation in KO mice in the context of an adaptive behavioral response, we analyzed pCREB staining in KO and WT mice after restraint-stress. This stimulus is associated with immediate-early activation gene expression in several brain regions, including the cerebral cortex and the hippocampus (Melia et al., 1994; Cullinan et al., 1995) and proceeds by an NMDA-dependent mechanism consistent with activation of Ca^{2+}-dependent gene expression (Titze-de-Almeida et al., 1994; Bozas et al., 1997). WT animals subjected to 30 min of restraint-stress exhibited heightened pCREB staining in several brain regions, including the hippocampus (dentate, CA1, and CA3 areas) and cerebral cortex, relative to unrestrained animals (Fig. 8*A*). pCREB staining was most prominent immediately after the restraint-stress period and declined by 2 hr thereafter (Fig. 8*A*). In contrast, pCREB immunoreactivity after restraint-stress was consistently and significantly decreased in cortical neurons ($p < 0.0001$; n = 3 mice each for WT and KO groups) and in hippocampal CA1 neurons ($p = 0.0038$) of KO mice as compared with WT littermate controls (Fig. 8*A*,*C*). pCREB immunoreactivity was also decreased in CA3 neurons, but this decrease was marginally nonsignificant ($p = 0.083$). Expression of c-Fos was also examined as a marker of Ca^{2+}- and CREB-dependent gene expression. c-Fos immunoreactivity was observed in several brain regions of restraint-stressed WT mice, including cerebral cortex and hippocampus, but was profoundly deficient in KO mice (Fig. 8*B*). Neurons of the somatosensory cortex of KO mice appeared to be the most severely affected, with virtually no c-Fos immunoreactivity observed in these cells as compared with their counterparts in WT littermates (Fig. 8*B*). The impact of CaMKIV/Gr deficiency was region-specific in that no significant differences in pCREB expression were observed in some other brain regions, such as the amygdala (Fig. 8*C*). These results identified CaMKIV/Gr as a physiologically relevant CREB kinase that may operate in a brain region-specific manner.

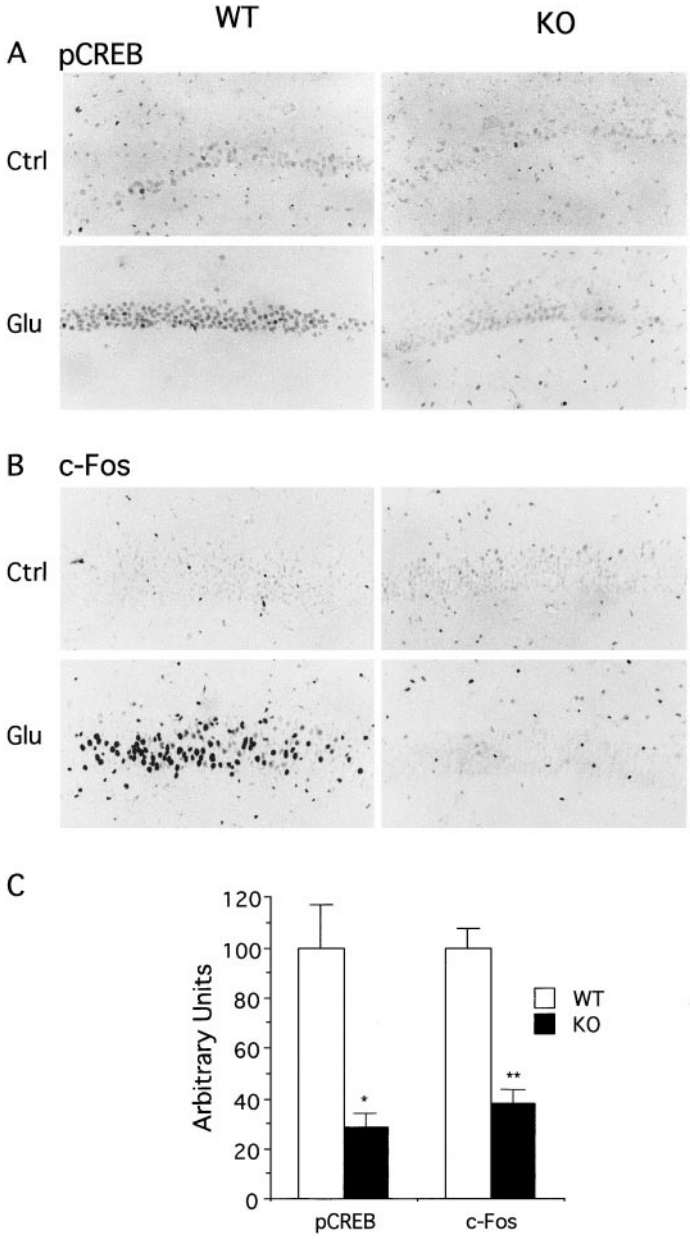

Figure 7. Decreased pCREB and c-Fos staining of CA1 neurons of glutamate-perfused hippocampal slices of CaMKIV/Gr KO mice compared with WT littermates. *A*, *B*, pCREB and c-Fos staining. Representative sections (20×) through the CA1 area of WT and KO hippocampal slices either left untreated (*Ctrl*) or subjected to glutamate perfusion for 45 min (*Glu*) are shown. Slices were stained with a pCREB (*A*) or c-Fos (*B*) antibody. Positive cells are demonstrated by deposition of a dark nuclear precipitate after peroxidase staining. *C*, Quantitation of pCREB and c-Fos immunohistochemistry of glutamate-treated slices. Densitometric analysis of sections from $n = 4$ WT and KO mice is shown. $^{*}p = 0.007$; $^{**}p < 0001$.

CaMKIV/Gr KO mice exhibit normal locomotion and sensorimotor functions but decreased walking initiation

To characterize the behavioral phenotype of CaMKIV/Gr KO mice, they and control WT littermates were first evaluated on a 1 hr locomotor activity test and a battery of sensorimotor tests, including ledge, platform, inclined screen, and walking initiation (Brosnan-Watters et al., 1996; Chiesa et al., 1998). Results of ANOVAs conducted on test variables indicated that the groups performed similarly on the 1 hr locomotor activity, ledge, platform, and inclined screen tests (data not shown). However, they differed significantly in their performance on the walking initiation test ($F_{(1,24)} = 8.51, p = 0.008$) (Fig. 9*A*). Subsequent contrasts indicated that the KO mice took significantly longer to leave the square compared with the WT mice on the first test session, ($F_{(1,24)} = 4.49$, $p = 0.045$). The KO mice also took longer to leave the square on test session 2, but these differences only approached significance ($F_{(1,24)} = 3.50, p = 0.074$).

The general coordination and motor skills of KO mice were further evaluated by testing them on a rotating rod (rotorod) that gradually increased its rotational speed over time. During the first (habituation/adaptation) phase of training, the KO and WT groups performed equally well in learning how to maintain their balance,

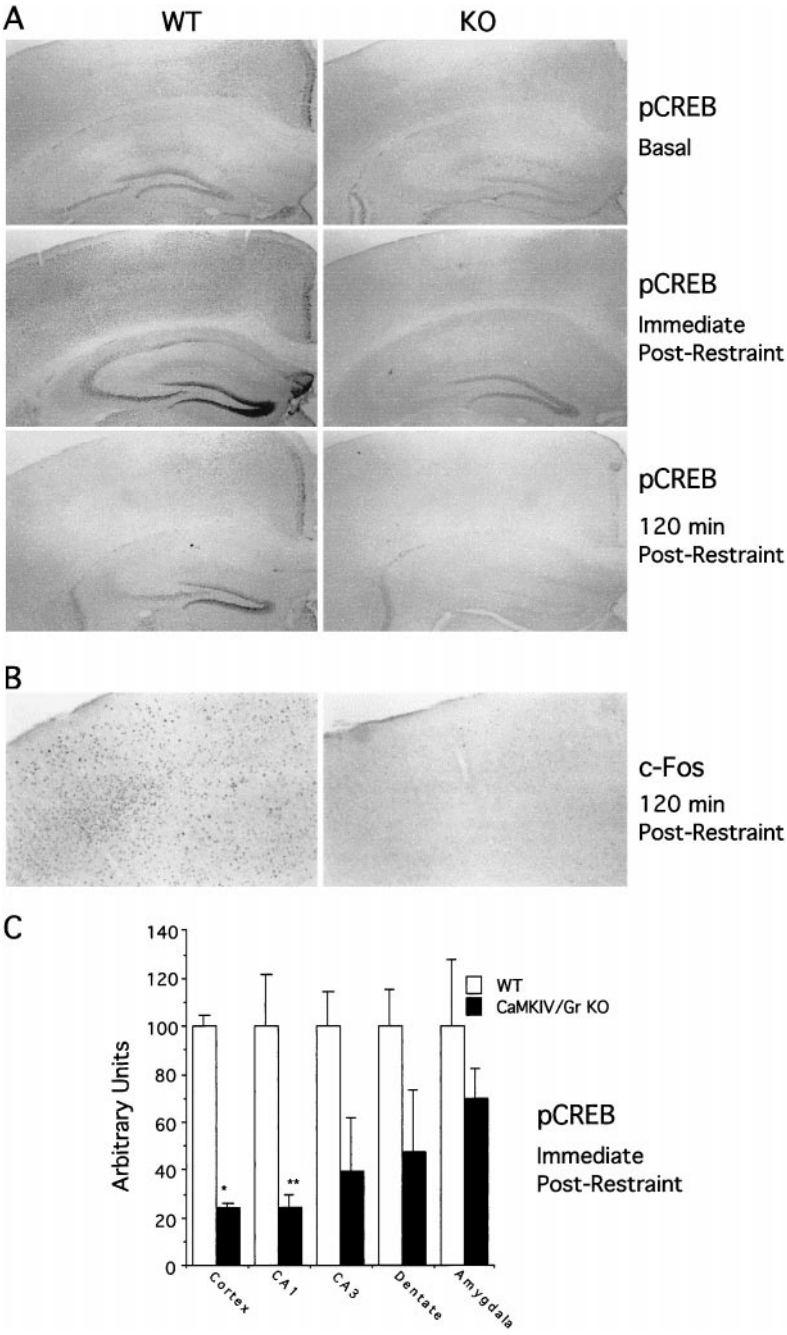

Figure 8. Decreased pCREB and c-Fos staining in brain subregions of restrain-stressed CaMKIV/Gr KO mice compared with WT littermate controls. *A*, pCREB staining. Representative sections (4× magnification) through the hippocampus of CaMKIV/Gr KO and WT mice left unmanipulated (*Basal*), immediately after 30 min of restraint-stress (*Immediate Post-Restraint*) or 2 hr thereafter (*120 min Post-Restraint*). Positive cells are demonstrated by deposition of a dark nuclear precipitate after peroxidase staining. *B*, c-Fos staining. Representative sections (10× magnification) through the somatosensory cortex of CaMKIV/Gr KO and WT mice 2 hr after restraint-stress. *C*, Quantitation of pCREB immunohistochemistry of sections obtained immediately post-restraint. Densitometric analysis of sections from $n = 3$ WT and KO mice is shown. $^{*}p < 0.0001$; $^{**}p = 0.038$.

first on a stationary rod and then on the same rod that was rotated at a slow constant speed (data not shown). The data from the accelerating rod condition are shown in Figure 9*B* and reveal that the two groups performed similarly during the accelerating rod condition. The performance of the two groups gradually improved over the 5 d test period, indicative of enhancement of motor skills with practice. This was confirmed by an ANOVA of these data that yielded a nonsignificant main effect of group and a significant effect of test days ($F_{(4,76)} = 4.61$, $p = 0.008$).

CaMKIV/Gr KO mice are not impaired in tests of spatial memory

Because impaired LTP in CA1 neurons has frequently been associated with poor spatial memory, we examined the performance of CaMKIV/Gr KO mice in two tests of spatial learning and memory: the Morris water maze and the eight-arm radial maze tests (Olton et al., 1978; Morris et al., 1982). The Morris water navigation task was used to evaluate spatial reference memory during cued (visible platform), place (submerged platform), and reversal trials (submerged platform in a different location). Cued training was also included to determine whether nonassociative factors were likely to confound interpretation of spatial learning/memory performance. To enhance the sensitivity of the test, we increased the degree of difficulty of the reversal trials relative to that of the place trials by substantially increasing the interval between the second and third trials from ~35 sec to 1 hr.

Figure 10 depicts the escape latency (*A*) and path length data (*B*) as a function of blocks of trials for the cued, place, and reversal trials. Results of ANOVAs conducted on these data revealed that the KO mice and WT littermate controls performed similarly on all three types of trials. Both groups showing steep learning curves on the cued and reversal trials, indicating substantial improvement over trial blocks for both latency and path length. In addition, the results of analyses on mean daily swimming speed scores showed that the KO and WT mice did not differ on this variable during cued, place, or reversal trials. These findings further substantiate the escape latency and path length data from the cued trials

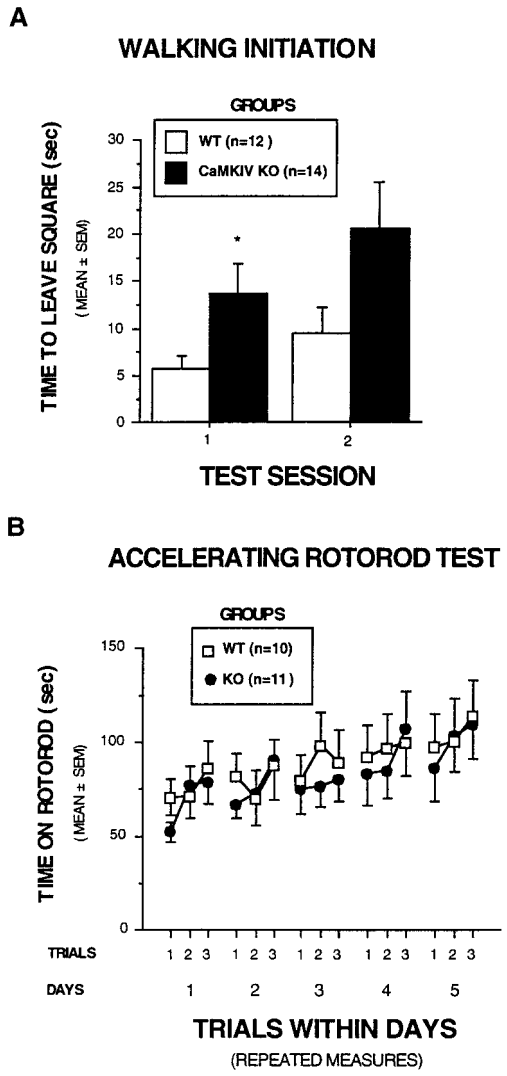

Figure 9. Performance of CaMKIV/Gr KO mice and WT littermate controls on walking initiation and accelerated rotorod testing. *A*, Walking initiation test. Results of the walking initiation test portion of the sensorimotor battery are shown, demonstrating that CaMKIV/Gr mice consistently took longer to leave the square than the WT mice. An ANOVA of these data revealed a significant main effect of group ($p = 0.008$). Subsequent pairwise comparisons showed that the groups differed significantly (*) on the first test session ($p = 0.045$), whereas differences only approached significance on the second session ($p = 0.074$). See Results for additional details of the statistical analyses. *B*, Accelerated rotorod test. Results show that the two groups of mice performed similarly on the accelerating rotorod, suggesting that the CaMKIV/Gr KO mice were not impaired in terms of general coordination and motor skills. However, there was a main effect of test days ($p = 0.035$), suggesting that the groups improved their performance over time.

suggesting that the KO and WT mice did not differ in terms of swimming capabilities.

With regard to the probe trials, Figure 10*C* shows that the KO mice and their WT littermate controls performed similarly in terms of platform crossings on the first probe trial during place training. Although the KO mice improved their performance on the second probe trial during place training, the two groups did not differ, however, in terms of their performance. A similar pattern of results was found when the time spent in the target quadrant (Fig. 10*D*) or the percentage of the total distance traveled in the target quadrant (data not shown) served as the dependent variables.

In contrast to the probe trial findings during place training was the performance of the two groups of mice on the first probe trial during reversal training. With regard to platform crossings, the KO mice performed significantly better (i.e., exhibited more platform crossings) than the WT mice ($F_{(1,24)} = 5.20$, $p = 0.032$) (Fig. 10*C*). The KO mice also tended to perform better than the WT mice with respect to the time spent in the target quadrant with the differences being marginally nonsignificant ($F_{(1,24)} = 3.90$, $p = 0.060$) (Fig. 10*D*). The second probe trial associated with reversal training was conducted 3 d after the last reversal trial to make the probe test more difficult by increasing the retention interval between the last training trial and the subsequent (second) probe trial. When the mice were tested on the second probe trial associated with reversal training, the KO and WT mice performed very similarly with regard to both platform crossings and time spent in the target quadrant (Fig. 10*C*,*D*).

We next tested CaMKIV/Gr KO mice and WT littermate controls on a win-shift spatial discrimination in the radial arm maze, which provided a measure of working (trial-dependent) memory capacities (Olton et al., 1978). We also evaluated neophobia (avoidance of a familiar food in a novel environment) and the time required to reach a criterion signifying "habituation" to assess the possibility that differences in emotionality between the groups might affect acquisition performance. Figure 11*A* shows that the KO mice took longer to begin eating in the radial maze compared with the WT mice on both test days. Results of the two-way ANOVA on the neophobia data indicated that there was a marginally nonsignificant main effect of group ($F_{(1,22)} = 4.18$, $p = 0.053$), a significant main effect of test day ($F_{(1,22)} = 7.26$, $p = 0.013$), and a nonsignificant group by test day interaction. KO mice took significantly longer to begin eating on test day 2 ($F_{(1,22)} = 5.49$, $p = 0.029$), whereas differences observed on test day 1 were nonsignificant. Data pertaining to habituation and acquisition are depicted in Figure 11*B–D*, which shows that the habituation and acquisition performance of the two groups was very similar. The WT and KO mice did not differ in terms of the number of days required to reach the habituation or acquisition criteria or on the number of errors (retracing) to criterion during acquisition.

DISCUSSION

CaMKIV/Gr and synaptic plasticity

By using mutant mice derived by targeted gene disruption, an important role for CaMKIV/Gr was demonstrated in hippocampal and cerebellar synaptic plasticity and in neuronal CREB activation. In CA1 neurons, LTP formation depends on Ca^{2+} influx via NMDA receptor channels. Although the function of these channels in KO mice appeared intact, nevertheless at least some of the downstream Ca^{2+}-dependent cellular signaling cascades were affected by CaMKIV/Gr deficiency, as evidenced by failure to induce sustained potentiation (L-LTP) after multiple-train high-frequency tetanization and by impaired CREB activation and Ca^{2+}-dependent gene transcription. In contrast, a transient form of synaptic potentiation (E-LTP) induced by a single tetanization was unimpaired. On the basis of previous studies documenting the dependence of L-LTP but not E-LTP on CREB activation and on *de novo* protein synthesis, defective CREB activation and Ca^{2+}- and CREB-dependent gene transcription may contribute to the failure of LTP to persist in repeatedly tetanized CA1 neurons of KO mice (Frey et al., 1988, 1993; Bourtchuladze et al., 1994; Huang and Kandel, 1994). However, it should be noted that the defect in L-LTP induction is notable very early (within the first 5 min) after both two- and four-train tetanization, at which time gene expression is unlikely to be involved in LTP formation. This would suggest a contribution by CaMKIV/Gr to early events in L-LTP formation independent of Ca^{2+} influx-triggered gene expression.

One nontranscriptional mechanism by which CaMKIV/Gr may contribute to L-LTP could involve phosphorylation by resident kinase molecules at postsynaptic densities of ion channels, cytoskeletal proteins, and their regulators. A precedent for ion channel phosphorylation as a contributing mechanism to LTP formation is provided by the case of CaMKII, which phosphorylates Ser-831 of GluR1 subunits of AMPA channels to promote channel conductance (Barria et al., 1997a,b; Derkach et al., 1999). Modulation of

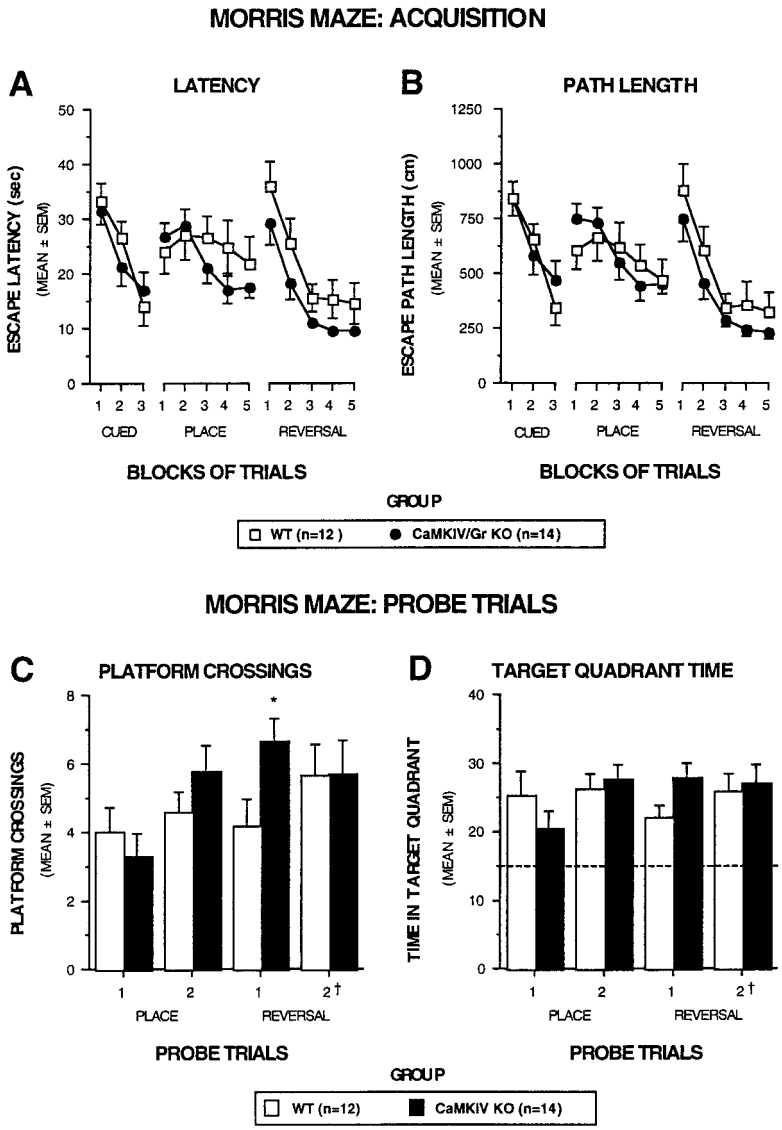

Figure 10. CaMKIV/Gr KO mice performed similarly to WT littermates on several aspects of the Morris water navigation task. *A*, *B*, Acquisition performance in terms of escape latency and path length is depicted for the cued, place, and reversal conditions as a function of blocks of trials. No differences were found between the groups during any of these conditions with regard to either escape latency (*A*) or path length (*B*). *C*, *D*, Retention performance on probe trials is shown. During the probe trials the mice were placed in the pool with the platform removed, and aspects of searching behavior were quantified over a 60 sec period. During place training, no differences were found between KO and WT mice in terms of the number of times the mice swam over the former platform location (*C*, *PLATFORM CROSSINGS*) or in the amount of time the mice spent searching in the quadrant where the platform used to be located (*D*, *TARGET QUADRANT TIME*). However, the CaMKIV/Gr KO mice exhibited a significantly (*) greater number of platform crossings on the first probe trial during reversal training ($p = 0.03$) and also tended to spend more time in the target quadrant (*D*), although the difference was marginally nonsignificant ($p = 0.06$). In *D* the *dotted line* represents the amount of time spent in the target quadrant that would be expected on the basis of chance alone. In addition, † signifies that the second probe trial associated with the reversal condition actually occurred 3 d after the completion of reversal training.

cytoskeletal protein function provides another mechanism by which CaMK may stabilize dendritic spines at synapses. The previous demonstration that CaMKIV/Gr promotes microtubule assembly by phosphorylating the microtubule regulator stathmin/OP18 illustrates one potential mechanism by which CaMKIV/Gr may regulate synaptic architecture and promote synaptic plasticity (Melander Gradin et al., 1997).

The finding that the late phase of cerebellar LTD was suppressed in cultured Purkinje neurons derived from CaMKIV/Gr KO mice suggests that CaMKIV/Gr is necessary for the expression of the late phase. This is consistent with previous findings that the late phase of cerebellar LTD could be blocked by nonspecific CaMK inhibitors (which do not distinguish between CaMKII and CaMKIV), two different dominant-negative CaMKIV constructs, or expression of a nuclear calmodulin trap (Ahn et al., 1999). It is also consistent with the previous demonstration that the late phase of cerebellar LTD is CREB dependent (Ahn et al., 1999). However, there are some limitations to the interpretation of these results that should be noted. First, some aspects of the basal physiology of the *in vitro* cultured CaMKIV/Gr KO Purkinje neurons are clearly abnormal. The frequency of mEPSCs is reduced and R_{input} is increased, both consistent with a reduction in the extent of the dendritic arbor of *in vitro* cultured Purkinje neurons. Although there is no particular reason to believe that the *in vitro* alterations suppress a late phase of LTD through nonspecific mechanisms, this possibility cannot be ignored entirely. Second, although CaMKIV/Gr is strongly expressed in the nucleus of neonatal Purkinje neurons, adult Purkinje neurons express CaMKIV/Gr only weakly (Sakagami et al., 1992; Sakagami and Kondo, 1993a), suggesting that this pathway may not necessarily underlie a late phase of cerebellar LTD throughout the life span.

CaMKIV/Gr, pCREB, and Ca^{2+}-dependent gene transcription

The demonstration of profoundly impaired CREB activation and Ca^{2+}-dependent gene transcription in some brain subregions of CaMKIV/Gr KO mice, including the hippocampus and cerebral cortex, is consistent with a prominent role played by CaMKIV/Gr in mediating these activation events. Nevertheless, CaMKIV/Gr is but one of several activators of CREB implicated in neuronal plasticity and adaptive behavioral responses, raising the issue of unique and redundant functions of the respective kinase. The differential impact of CaMKIV/Gr deficiency on CREB phosphorylation in brain regions of restraint-stressed animals suggests that under at least some conditions CREB activators such as CaMKIV/Gr may be used selectively in a tissue-specific manner. It is also possible that different CREB activators may function over distinct time periods. For example, it has been suggested previously that CaMKIV/Gr, by virtue of its constitutive nuclear expression and its amenability to activation by fast-moving Ca^{2+} waves generated at distal synapses, may drive fast-onset CREB activation, whereas other activators such as cAMP/PKA or cascading

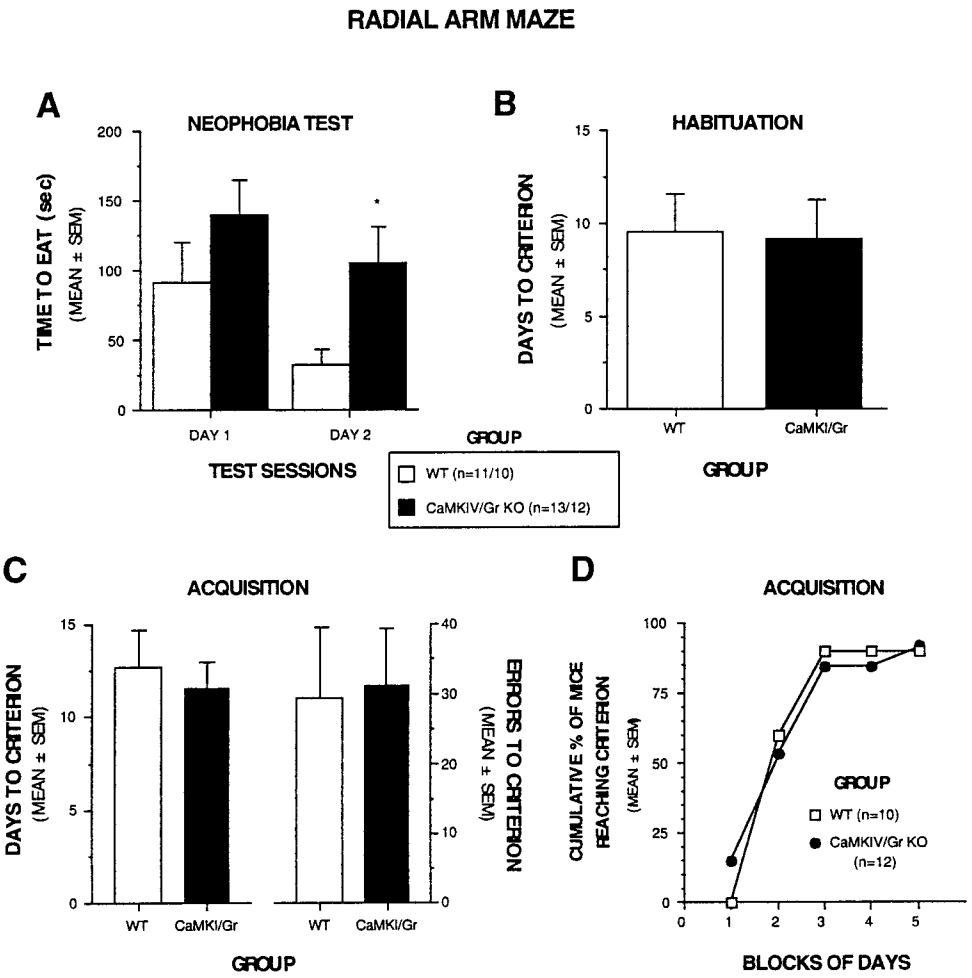

Figure 11. Performance of CaMKIV/Gr and WT mice on the radial arm maze. *A*, Neophobia. CaMKIV/Gr KO mice tended to take longer to begin eating the food reward in the radial arm maze during the first 2 d of habituation compared with the WT littermate controls ($F_{(1,22)} = 4.18$, $p = 0.053$). Pairwise comparisons conducted within each test day indicated that the CaMKIV/Gr mice took significantly (*) longer to begin eating in the maze on day 2 relative to the WT mice ($F_{(1,22)} = 5.49$, $p = 0.029$). *B*, Habituation. Although the CaMKIV/Gr-deficient mice were more reluctant to eat the food reward during the early portions of the habituation compared with the WT mice, the two groups required similar amounts of time to reach criterion for terminating habituation. *C*, *D*, Acquisition results. The acquisition performance was not significantly different between the groups in terms of either days or errors to criterion (*C*). The acquisition performance of the two groups of mice over time is depicted in *D*, which shows that groups exhibited similar rates of learning in terms of the cumulative percentage of mice reaching criterion as a function of blocks of 6 d.

mitogen-activated protein kinases may activate CREB more slowly (Finkbeiner et al., 1997). Comparative studies on spatial and temporal aspects of CREB activation in animals lacking different CREB activators (and combinations thereof) may provide further insight into unique, redundant, and integrated functions of these pathways.

CaMKIV/Gr in learning and memory

Although LTP formation, CREB activation, and Ca^{2+}-dependent gene transcription were all impaired in CA1 neurons of CaMKIV/Gr KO mice, there was no evidence of disturbed spatial learning in the CaMKIV/Gr KO mice compared with WT controls. A relationship between CA1 LTP and spatial memory was surmised from studies on NMDA receptor- and CaMKIIα-deficient mice, and more recently from studies on mice deficient in other molecules involved in LTP formation such as TrkB (Silva et al., 1992a,b; Tsien et al., 1996; Minichiello et al., 1999). However, deficiency of other molecules, such as AMPA channels, that results in LTP deficiency is not associated with impaired learning in the Morris water maze (Zamanillo et al., 1999). It is possible that the short- and long-term forms of LTP spared by the mutation are sufficient to support spatial learning by CaMKIV/Gr KO mice. An alternative explanation, suggested by the findings of Zamanillo et al. (1999), may be that LTP is not necessary for spatial learning and memory in the context of the Morris water maze and the radial arm maze tasks. In the case of CREB, it is possible that CREB phosphorylation may still proceed during spatial memory induction by pathways other than those invoked in our pCREB studies (KCl depolarization, glutamate stimulation, restraint-stress). An alternative explanation that we favor is that residual CREB activation in CA1 neurons of CaMKIV/Gr KO mice may be sufficient to rescue spatial memory. This would be consistent with the finding that the impact of CREB deficiency on LTM is gene dosage dependent (Gass et al., 1998). If so, then it could be predicted that combined deficiency of CaMKIV/Gr and other Ca^{2+}-regulated CREB activating pathways such as ACI or ACVIII, the deficiency of which does not perturb spatial memory (Wong et al., 1999), may sufficiently compromise CREB activation to precipitate spatial memory defects.

Although testing on the Morris water navigation task revealed no evidence of impaired spatial learning or memory in CaMKIV/Gr KO mice, it should be noted that other investigators have reported that certain training conditions may reveal impairments in spatial learning in mice that have CREB deficits (Bourtchuladze et al., 1994; Kogan et al., 1997; Gass et al., 1998). Kogan et al. (1997) reported that the inter-trial interval was an important parameter for demonstrating place learning deficits in CREB mutant mice because impairment was demonstrable when the inter-trial interval was 1 min but not when it was 10 min in duration. However, it is unlikely that this factor can account for the lack of impairment observed in CaMKIV/Gr KO mice during place training on the water navigation task in the present study because a very short inter-trial interval (35 sec) was used.

In addition to their apparently intact spatial memory, CaMKIV/Gr KO mice were also found to be no different from WT controls in terms of general coordination and motor skills. This was attested to by the performance of KO mice in the ledge, plank, platform, and rotorod tests as well as the lack of differences in swimming speeds and cued learning performance during the Morris water navigation task. KO mice also demonstrated improved performance on the rotorod test as a function of practice, suggesting that at least some forms of motor learning are intact. Nevertheless, the absence in KO mice of a late form of cerebellar LTD

suggests that CaMKIV/Gr may contribute to aspects of motor learning that are dependent on cerebellar LTD formation, such as associative eye blink conditioning and adaptation of the vestibulo-occular reflex (Daniel et al., 1998). Further studies will be required to determine the role of CaMKIV/Gr in cerebellar LTD-dependent motor learning paradigms.

Finally, impaired performance of CaMKIV/Gr KO mice on the walking initiation test and their failure to rapidly habituate to the fear of eating in a novel environment (neophobia) in the radial arm maze test suggest altered emotionality of the mutant mice compared with their littermate controls (Wozniak et al., 1990; Brosnan-Watters et al., 1996). In light of this premise, it will be interesting to explore the possibility that these mice are impaired on learning tasks that contain a component relating to changes in emotionality.

REFERENCES

Abel T, Nguyen PV, Barad M, Deuel TA, Kandel ER, Bourtchouladze R (1997) Genetic demonstration of a role for PKA in the late phase of LTP and in hippocampus-based long-term memory. Cell 88:615–626.

Ahn S, Ginty DD, Linden DJ (1999) A late phase of cerebellar long-term depression requires activation of CaMKIV and CREB. Neuron 23:559–568.

Bach ME, Hawkins RD, Osman M, Kandel ER, Mayford M (1995) Impairment of spatial but not contextual memory in CaMKII mutant mice with a selective loss of hippocampal LTP in the range of the theta frequency. Cell 81:905–915.

Barria A, Derkach V, Soderling T (1997a) Identification of the Ca^{2+}/calmodulin-dependent protein kinase II regulatory phosphorylation site in the alpha-amino-3-hydroxyl-5-methyl-4-isoxazole-propionate-type glutamate receptor. J Biol Chem 272:32727–32730.

Barria A, Muller D, Derkach V, Griffith LC, Soderling TR (1997b) Regulatory phosphorylation of AMPA-type glutamate receptors by CaMKII during long-term potentiation. Science 276:2042–2045.

Bito H, Deisseroth K, Tsien RW (1996) CREB phosphorylation and dephosphorylation: a Ca^{2+}-and stimulus duration-dependent switch for hippocampal gene expression. Cell 87:1203–1214.

Blaeser F, Ho N, Prywes R, Chatila TA (2000) Ca^{2+}-dependent gene transcription mediated by MEF2 transcription factors. J Biol Chem 275:197–209.

Bourtchuladze R, Frenguelli B, Blendy J, Cioffi D, Schutz G, Silva AJ (1994) Deficient long-term memory in mice with a targeted mutation of the cAMP-responsive element-binding protein. Cell 79:59–68.

Bozas E, Tritos N, Phillipidis H, Stylianopoulou F (1997) At least three neurotransmitter systems mediate a stress-induced increase in c-fos mRNA in different rat brain areas. Cell Mol Neurobiol 17:157–169.

Brandon EP, Zhuo M, Huang YY, Qi M, Gerhold KA, Burton KA, Kandel ER, McKnight GS, Idzerda RL (1995) Hippocampal long-term depression and depotentiation are defective in mice carrying a targeted disruption of the gene encoding the RI beta subunit of cAMP-dependent protein kinase. Proc Natl Acad Sci USA 92:8851–8855.

Brosnan-Watters G, Wozniak DF, Nardi A, Olney JW (1996) Acute behavioral effects of MK-801 in the mouse. Pharmacol Biochem Behav 53:701–711.

Brosnan-Watters G, Wozniak DF, Nardi A, Olney JW (1999) Parallel recovery of MK-801-induced spatial learning impairment and neuronal injury in male mice. Pharmacol Biochem Behav 62:111–122.

Chatila T, Anderson KA, Ho N, Means AR (1996) A unique phosphorylation-dependent mechanism for the activation of Ca^{2+}/calmodulin-dependent protein kinase type IV/GR. J Biol Chem 271:21542–21548.

Chawla S, Hardingham GE, Quinn DR, Bading H (1998) CBP: a signal-regulated transcriptional coactivator controlled by nuclear calcium and CaM kinase IV. Science 281:1505–1509.

Chen C, Tonegawa S (1997) Molecular genetic analysis of synaptic plasticity, activity-dependent neural development, learning, and memory in the mammalian brain. Annu Rev Neurosci 20:157–184.

Chiesa R, Piccardo P, Ghetti B, Harris DA (1998) Neurological illness in transgenic mice expressing a prion protein with an insertional mutation. Neuron 21:1339–1351.

Cho YH, Giese KP, Tanila H, Silva AJ, Eichenbaum H (1998) Abnormal hippocampal spatial representations in alphaCaMKIIT286A and CREBalphaDelta-mice. Science 279:867–869.

Cullinan WE, Herman JP, Battaglia DF, Akil H, Watson SJ (1995) Pattern and time course of immediate early gene expression in rat brain following acute stress. Neuroscience 64:477–505.

Daniel H, Levenes C, Crepel F (1998) Cellular mechanisms of cerebellar LTD. Trends Neurosci 21:401–407.

Derkach V, Barria A, Soderling TR (1999) Ca^{2+}/calmodulin-kinase II enhances channel conductance of alpha-amino-3-hydroxy-5-methyl-4-isoxazolepropionate type glutamate receptors. Proc Natl Acad Sci USA 96:3269–3274.

Dubnau J, Tully T (1998) Gene discovery in *Drosophila*: new insights for learning and memory. Annu Rev Neurosci 21:407–444.

Dudek SM, Bear MF (1992) Homosynaptic long-term depression in area CA1 of hippocampus and effects of *N*-methyl-D-aspartate receptor blockade. Proc Natl Acad Sci USA 89:4363–4367.

Dugan LL, Kim JS, Zhang Y, Bart RD, Sun Y, Holtzman DM, Gutmann DH (1999) Differential effects of cAMP in neurons and astrocytes. Role of B-raf. J Biol Chem 274:25842–25848.

Enslen H, Tokumitsu H, Stork PJ, Davis RJ, Soderling TR (1996) Regulation of mitogen-activated protein kinases by a calcium/calmodulin-dependent protein kinase cascade. Proc Natl Acad Sci USA 93:10803–10808.

Finkbeiner S, Tavazoie SF, Maloratsky A, Jacobs KM, Harris KM, Greenberg ME (1997) CREB: a major mediator of neuronal neurotrophin responses. Neuron 19:1031–1047.

Frey U, Huang YY, Kandel ER (1993) Effects of cAMP simulate a late stage of LTP in hippocampal CA1 neurons. Science 260:1661–1664.

Frey U, Krug M, Reymann KG, Matthies H (1988) Anisomycin, an inhibitor of protein synthesis, blocks late phases of LTP phenomena in the hippocampal CA1 region in vitro. Brain Res 452:57–65.

Gass P, Wolfer DP, Balschun D, Rudolph D, Frey U, Lipp HP, Schutz G (1998) Deficits in memory tasks of mice with CREB mutations depend on gene dosage. Learn Mem 5:274–288.

Giese KP, Fedorov NB, Filipkowski RK, Silva AJ (1998) Autophosphorylation at Thr286 of the alpha calcium-calmodulin kinase II in LTP and learning. Science 279:870–873.

Hu SC, Chrivia J, Ghosh A (1999) Regulation of CBP-mediated transcription by neuronal calcium signaling. Neuron 22:799–808.

Huang YY, Kandel ER (1994) Recruitment of long-lasting and protein kinase A-dependent long-term potentiation in the CA1 region of hippocampus requires repeated tetanization. Learn Mem 1:74–82.

Impey S, Obrietan K, Wong ST, Poser S, Yano S, Wayman G, Deloulme JC, Chan G, Storm DR (1998) Cross talk between ERK and PKA is required for Ca^{2+} stimulation of CREB-dependent transcription and ERK nuclear translocation. Neuron 21:869–883.

Jensen KF, Ohmstede CA, Fisher RS, Olin JK, Sahyoun N (1991a) Acquisition and loss of a neuronal Ca^{2+}/calmodulin-dependent protein kinase during neuronal differentiation. Proc Natl Acad Sci USA 88:4050–4053.

Jensen KF, Ohmstede CA, Fisher RS, Sahyoun N (1991b) Nuclear and axonal localization of Ca^{2+}/calmodulin-dependent protein kinase type Gr in rat cerebellar cortex. Proc Natl Acad Sci USA 88:2850–2853.

Jones DA, Glod J, Wilson-Shaw D, Hahn WE, Sikela JM (1991) cDNA sequence and differential expression of the mouse Ca^{2+}/calmodulin dependent protein kinase IV gene. FEBS Lett 289:105–109.

Kogan JH, Frankland PW, Blendy JA, Coblentz J, Marowitz Z, Schutz G, Silva AJ (1997) Spaced training induces normal long-term memory in CREB mutant mice. Curr Biol 7:1–11.

Linden DJ (1996) A protein synthesis-dependent late phase of cerebellar long-term depression. Neuron 17:483–490.

Mathews RP, Guthrie CR, Wailes LM, Zhao X, Means AR, Mcknight GS (1994) Calcium/calmodulin-dependent protein kinase types II and IV differentially regulate CREB-dependent gene expression. Mol Cell Biol 14:6107–6116.

Mayford M, Bach ME, Huang YY, Wang L, Hawkins RD, Kandel ER (1996) Control of memory formation through regulated expression of a CaMKII transgene. Science 274:1678–1683.

Mayford M, Kandel ER (1999) Genetic approaches to memory storage. Trends Genet 15:463–470.

Means AR, Cruzalegui F, LeMagueresse B, Needleman DS, Slaughter GR, Ono T (1991) A novel Ca^{2+}/calmodulin-dependent protein kinase and a male germ cell-specific calmodulin-binding protein are derived from the same gene. Mol Cell Biol 11:3960–3971.

Melander Gradin H, Marklund U, Larsson N, Chatila TA, Gullberg M (1997) Regulation of microtubule dynamics by Ca^{2+}/calmodulin-dependent kinase IV/Gr-dependent phosphorylation of oncoprotein 18. Mol Cell Biol 17:3459–3467.

Melia KR, Ryabinin AE, Schroeder R, Bloom FE, Wilson MC (1994) Induction and habituation of immediate early gene expression in rat brain by acute and repeated restraint-stress. J Neurosci 14:5929–5938.

Minichiello L, Korte M, Wolfer D, Kuhn R, Unsicker K, Cestari V, Rossi-Arnaud C, Lipp HP, Bonhoeffer T, Klein R (1999) Essential role for TrkB receptors in hippocampus-mediated learning. Neuron 24:401–414.

Miranti CK, Ginty DD, Huang G, Chatila T, Greenberg M (1995) Calcium activates serum response factor-dependent transcription by a ras and Elk-1-independent mechanism that involves a CaM kinase. Mol Cell Biol 15:3672–3684.

Morris RG, Garrud P, Rawlins JN, O'Keefe J (1982) Place navigation impaired in rats with hippocampal lesions. Nature 297:681–683.

Murashima M, Hirano T (1999) Entire course and distinct phases of day-lasting depression of miniature EPSC amplitudes in cultured Purkinje neurons. J Neurosci 19:7326–7333.

Nguyen PV, Abel T, Kandel ER (1994) Requirement of a critical period of transcription for induction of a late phase of LTP. Science 265:1104–1107.

Ohmstede C-A, Bland MM, Merrill BM, Sahyoun N (1991) Relationship of genes encoding Ca^{2+}/calmodulin-dependent protein kinase Gr and calspermin: a gene within a gene. Proc Natl Acad Sci USA 88:5784–5788.

Ohmstede C-A, Jensen KF, Sahyoun NE (1989) Ca^{2+}/calmodulin-dependent protein kinase enriched in cerebellar granule cells. J Biol Chem 264:5866–5875.

Olton DS, Walker JA, Gage FH (1978) Hippocampal connections and spatial discrimination. Brain Res 139:295–308.

Qi M, Zhuo M, Skalhegg BS, Brandon EP, Kandel ER, McKnight GS, Idzerda RL (1996) Impaired hippocampal plasticity in mice lacking the Cbeta1 catalytic subunit of cAMP-dependent protein kinase. Proc Natl Acad Sci USA 93:1571–1576.

Sakagami H, Kondo H (1993) Cloning and sequencing of a gene encoding the beta polypeptide of Ca^{2+}/calmodulin-dependent protein kinase IV and its expression confined to the mature cerebellar granule cells. Brain Res Mol Brain Res 19:215–218.

Sakagami H, Watanabe M, Kondo H (1992) Gene expression of Ca^{2+}/calmodulin-dependent protein kinase of the cerebellar granule cell type or type IV in the mature and developing rat brain. Brain Res Mol Brain Res 16:20–28.

Shaywitz AJ, Greenberg ME (1999) CREB: a stimulus-induced transcription factor activated by a diverse array of extracellular signals. Annu Rev Biochem 68:821–861.

Shieh PB, Hu SC, Bobb K, Timmusk T, Ghosh A (1998) Identification of a signaling pathway involved in calcium regulation of BDNF expression. Neuron 20:727–740.

Silva AJ, Kogan JH, Frankland PW, Kida S (1998) CREB and memory. Annu Rev Neurosci 21:127–148.

Silva AJ, Paylor R, Wehner JM, Tonegawa S (1992a) Impaired spatial learning in alpha-calcium-calmodulin kinase II mutant mice. Science 257:206–211.

Silva AJ, Stevens CF, Tonegawa S, Wang Y (1992b) Deficient hippocampal long-term potentiation in alpha-calcium-calmodulin kinase II mutant mice. Science 257:201–206.

Sun P, Enslen H, Myung PS, Maurer RA (1994) Differential activation of CREB by Ca^{2+}/calmodulin-dependent protein kinases type II and type IV involves phosphorylation of a site that negatively regulates activity. Genes Dev 8:2527–2539.

Sun P, Lou L, Maurer RA (1996) Regulation of activating transcription factor-1 and the cAMP response element-binding protein by Ca^{2+}/calmodulin-dependent protein kinases type I, II, and IV. J Biol Chem 271:3066–3073.

Sun Z, means RL, LeMagueresse B, Means AR (1995) Organization and analysis of the complete rat calmodulin-dependent protein kinase IV gene. J Biol Chem 270:29507–29514.

Tao X, Finkbeiner S, Arnold DB, Shaywitz AJ, Greenberg ME (1998) Ca^{2+} influx regulates BDNF transcription by a CREB family transcription factor-dependent mechanism. Neuron [Erratum (1998) 20:1297] 20:709–726.

Titze-de-Almeida R, de Oliveira CL, Shida HW, Guimaraes FS, Del Bel EA (1994) Midazolam and the *N*-methyl-D-aspartate (NMDA) receptor antagonist 2-amino-7-phosphonoheptanoic acid (AP-7) attenuate stress-induced expression of c-fos mRNA in the dentate gyrus. Cell Mol Neurobiol 14:373–380.

Tsien JZ, Huerta PT, Tonegawa S (1996) The essential role of hippocampal CA1 NMDA receptor-dependent synaptic plasticity in spatial memory. Cell 87:1327–1338.

Tybulewicz VLJ, Crawford CE, Jackson PK, Bronson RT, Mulligan RC (1991) Neonatal lethality and lymphopenia in mice with a homozygous disruption of the c-abl proto-oncogene. Cell 65:1153–1163.

Wong ST, Athos J, Figueroa XA, Pineda VV, Schaefer ML, Chavkin CC, Muglia LJ, Storm DR (1999) Calcium-stimulated adenylyl cyclase activity is critical for hippocampus-dependent long-term memory and late phase LTP. Neuron 23:787–798.

Wozniak DF, Olney JW, Kettinger L, Price M, Miller JP (1990) Behavioral effects of MK-801 in the rat. Psychopharmacology 101:47–56.

Zamanillo D, Sprengel R, Hvalby O, Jensen V, Burnashev N, Rozov A, Kaiser KM, Koster HJ, Borchardt T, Worley P, Lubke J, Frotscher M, Kelly PH, Sommer B, Andersen P, Seeburg PH, Sakmann B (1999) Importance of AMPA receptors for hippocampal synaptic plasticity but not for spatial learning. Science 284:1805–1811.

Zhuo M, Zhang W, Son H, Mansuy I, Sobel RA, Seidman J, Kandel ER (1999) A selective role of calcineurin alpha in synaptic depotentiation in hippocampus. Proc Natl Acad Sci USA 96:4650–4655.